FINAL REPORT

OSIRRUS: OCEANIC SYMBOLIC IMAGE REPRESENTATION, RECOGNITION AND UNDERSTANDING SOFTWARE

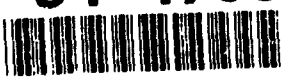

REPORT DOCUMENTATION PAGE

Form Approved
OBM No. 0704-0188

1. Agency Use Only *(Leave blank).*	2. Report Date. December 1990	3. Report Type and Dates Covered. Contractor Report -- Final

4. Title and Subtitle.
OSIRRUS: Oceanic Symbolic Image Representation, Recognition and Understanding Software

5. Funding Numbers.

Program Element No.	0602435N
Project No.	3587
Task No.	MOGO
Accession No.	DN259048
Work Unit No.	13210R

6. Author(s).
Lee A. Atkinson*

7. Performing Organization Name(s) and Address(es).
Consultant's Choice, Inc.
8800 Rowsell Road
Atlanta, GA 30350

8. Performing Organization Report Number.

9. Sponsoring/Monitoring Agency Name(s) and Address(es).
Naval Oceanographic and Atmospheric Research Laboratory
Ocean Sciences Directorate, Code 321
Stennis Space Center, MS 39529-5004

10. Sponsoring/Monitoring Agency Report Number.
CR 001:92

11. Supplementary Notes.
*Consultant's Choice, Inc., Atlanta, GA 30350
Contract Number N00014-89-C-6027

12a. Distribution/Availability Statement.
Approved for public release; distribution is unlimited.

12b. Distribution Code.

13. Abstract *(Maximum 200 words).*

Detection and proper labeling of oceanic mesoscale features in remotely sensed data is a mission of NOARL's Ocean Science Directorate. Automated identification of eddy rings and Gulf Stream walls (two oceanic mesoscale features of specific interest) in infrared satellite imagery using isotherm shape identification is a viable approach. This report presents the completion of work done by Consultant's Choice, Inc. (CCI), concentrating on eddy ring detection using shape identification and statistical analysis on detection features to reduce false alarms. An eddy ring is a large parcel of circulating ocean water, created from detached ocean stream undulations, having a trapped core of water whose temperature is markedly different from its surrounding waters. Warm eddy rings have warm cores, and cold eddy rings have cold cores.

Oceanic Symbolic Image Representation, Recognition and Understanding Software (OSIRRUS) converts imagery to a "symbolic form" in the sense that data are converted to a list of contiguous pixel points representing a contour of constant temperature on a thermal topology, which is termed an isotherm. Ideally, isotherms form characteristic shapes that envelop mesoscale features, such as eddy rings. Shapes identifying potential areas of interest are analyzed with an additional temperature profile to confirm eddy ring detection and provide automatically extracted measurements useful to a mission specialist.

14. Subject Terms.
Remote sensing, image segmentation, symbolic representation

15. Number of Pages.
51

16. Price Code.

17. Security Classification of Report.	18. Security Classification of This Page.	19. Security Classification of Abstract.	20. Limitation of Abstract.
Unclassified	Unclassified	Unclassified	SAR

SBIN/NORDA

FINAL REPORT
OSIRRUS: OCEANIC SYMBOLIC IMAGE REPRESENTATION, RECOGNITION AND UNDERSTANDING SOFTWARE

Contract No. N00014-89-C-6027

01 AUG 89 - 10 NOV 90

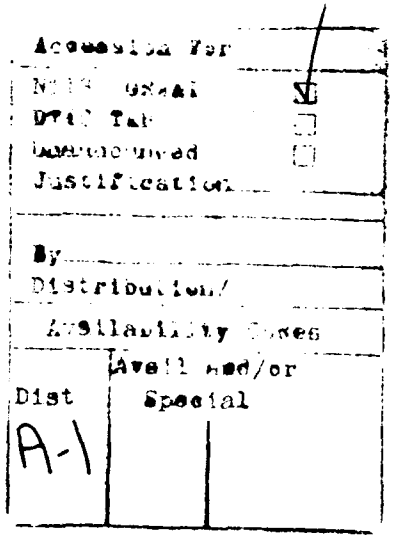

Prepared By

Lee A. Atkinson

of

Consultant's Choice, Inc.
8800 Roswell Road, Suie 130
Atlanta, Georgia 30350

for

Naval Oceanographic and Atmospheric
Research Laboratory (NOARL)
Department of the Navy
Stennis Space Center, MS 39529

December 1990

ACKNOWLEDGMENTS

This project was funded under contract to NOARL, Contract No. N00014-89-C-6027. The author wishes to express thanks to Matthew Lybanon for continued interest and support of OSIRRUS. Acknowledgments also go to Bennett Teates and Paul Lampru for acquisition and guidance, and to Kathie Speas for the manuscript and graphics.

TABLE OF CONTENTS

LIST OF FIGURES

LIST OF TABLES

OSIRRUS: OCEANIC SYMBOLIC IMAGE REPRESENTATION, RECOGNITION AND UNDERSTANDING SOFTWARE

1.0. INTRODUCTION

Detection and proper labeling of oceanic mesoscale features in remotely sensed data is a mission of NOARL's Ocean Science Directorate. Automated identification of eddy rings and Gulf Stream walls (two oceanic mesoscale features of specific interest) in infrared satellite imagery using isotherm shape identification is a viable approach. This report presents the completion of work done by Consultant's Choice, Inc. (CCI), concentrating on eddy ring detection, using shape identification and statistical analysis on detection features to reduce false alarms. An eddy ring is a large parcel of circulating ocean water, created from detached ocean stream undulations, having a trapped core of water whose temperature is markedly different from its surrounding waters. Warm eddy rings have warm cores, and cold eddy rings have cold cores.

Oceanic Symbolic Image Representation, Recognition and Understanding Software (OSIRRUS) converts imagery to a "symbolic form" in the sense that data are converted to a list of contiguous pixel points representing a contour of constant temperature on a thermal topology, which is termed an isotherm. Ideally, isotherms form characteristic shapes that envelop mesoscale features, such as eddy rings. Shapes identifying potential areas of interest are analyzed with an additional temperature profile to confirm eddy ring detection and provide automatically extracted measurements useful to a mission specialist.

Since isotherms are acquired easily for all thermal values in the image domain, OSIRRUS has the advantage of avoiding scale-dependent problems usually associated with feature-edge detection. Moreover, isotherms ensure unique labeling of edges (mixed labeling does not occur). OSIRRUS does not attempt to detect and label under one process. The technique of first performing shape extraction and then specific shape detection is more natural in the understanding of information presented, and leads to robust heuristics of detection and analysis. Also, since the techniques are separated, OSIRRUS has the capacity to detect and analyze a wider variety of thermal structures than using a finely-tuned specific detector. Even though shape recognition is of main interest, the isotherm representation still retains thermal information so that intelligent decisions using known physical and oceanographic properties may be made.

Isotherm extraction and identification involves processing of thousands of lists, each with varied lengths of possibly several hundred elements. Although difficult to manage in some programming environments, lists may be combined with data of varied form and type to form complex and powerful data structures. The development of OSIRRUS was performed on an Integrated Inference Machine (IIM)-Inferstar LISP machine capable of managing complex data structures in an interpretive environment with dynamic memory allocation and automatic variable typing. This platform allowed rapid prototyping of OSIRRUS and, therefore, rapid development of eddy ring shape identification. However, the algorithms that have been developed are not LISP nor LISP-machine specific, may be ported to the C language or assembly, and will operate on most microcomputers.

2.0 GENERAL METHOD

Described herein are the general steps (see Table I) for preprocessing, symbolic transformation, eddy ring detection, and detection analysis performed by OSIRRUS. Improvements concerning speed and quality of identification are described in Section 4.0.

TABLE I
GENERAL METHOD

STEP	OPERATIONS	TYPE	RESULT
1. PREPROCESSING	FILTER	SPATIAL	MEDIAN 5X5
	FILTER	SPATIAL	GAUSSIAN 5x5
2. IMAGE-TO-LIST XFORM	THRESHOLD	DOWN	BINARY
	EDGE	4 CONN	ISOTHERM IMAGE
	CONTOURIZE	RASTER SEARCH	ISOTHERM LIST
	FILTER	RULES	ISOTHERM LIST
	RECONNECT	SEARCH	ISOTHERM LIST
	FILTER	RULES	ISOTHERM LIST
3. DETECT-EDDYS	BOTTLENECK	RULES	BOTTLES
	RING FILTER	RULES	RINGS
4. DETECTION-ANALYSIS	GROUPING	CALC	FEATURE OBJECTS
	FEATURE ASSIGN	CALC	FEATURE OBJECTS

2.1 Preprocessing

OSIRRUS typically processes 256x256 pixel images with infrared intensity 0 to 255, representing coldest to warmest thermal signature, respectively. The original image is

processed using a median 5x5 filter to eliminate shot noise and ensure local continuity. This filter is best, since a median 3x3 does not filter typical images enough and a 7x7 does not gain much beyond a 5x5. It was found that, without this filter, many pygmy isotherms are created and large (long) isotherms are contaminated with spurious loops that do not yield general information about the thermal topology. To assist the median 5x5 filter, a Gaussian (binomial 5x5) filter evens out local small-scale features and digitization noise. While these two filters may lose information and gradient detail, feature shapes become much more apparent for recognition, and granularity of information is reduced.

2.2 Image-to-List Transformation

OSIRRUS transforms the preprocessed image into lists of isotherms by intensity levels. A given level (L) is processed to obtain all usable isotherms, and then the process is repeated for each intensity level. Isotherms from a given level or temperature are grouped together into a temperature-labeled list.

Assurance of unbroken isotherms is made by thresholding intensity values (T) to obtain a binary image (B) using the following rule:

$$\begin{aligned} T(x,y) > L \quad &\rightarrow \quad B(x,y) = 0 \\ T(x,y) \leq L \quad &\rightarrow \quad B(x,y) = 1 \end{aligned} \qquad (1)$$

Thresholding thus interpolates for areas where large gradients skip over intermediate intensity values. Isotherms are that set of pixels with intensity values not greater than L, which neighbor pixels with intensity levels greater than L (see Figure 1).

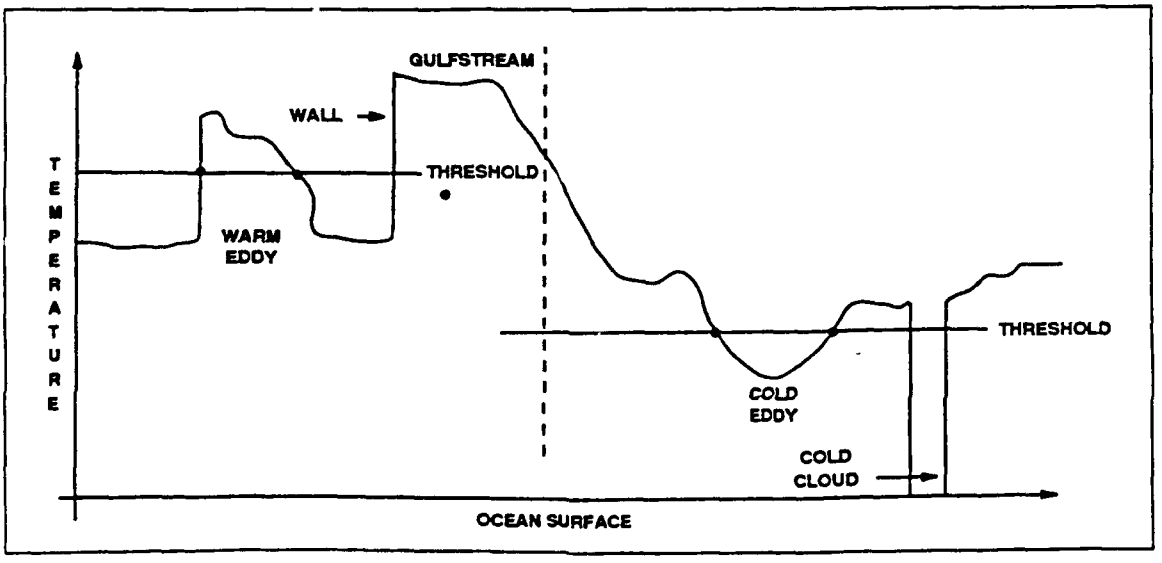

Figure 1. Thresholding for Contours (Isotherms)

Isotherms are formed from the resulting binary image B(x,y) by an edge operator. Edge pixels are only those pixels with a four-connected zero-valued neighbor. The simplest edge operator is the best! At this point, viewing the edge image results in display of image isotherms, revealing the shape of the thermal topography at the processed level (see Figure 2). The edge image is converted to symbolic format which is a list of lists of pixel coordinates, as illustrated in the LISP list below:

```
( ( (Xa Ya)  (Xb Yb)...(Xn Yn) )
  ( (Xc Yc)  (Xd Yd)...(Xm Ym) )
  .
  .
  .
  ( (Xe Ye)  (Xf Yf)...(Xp Yp) ) ).
```

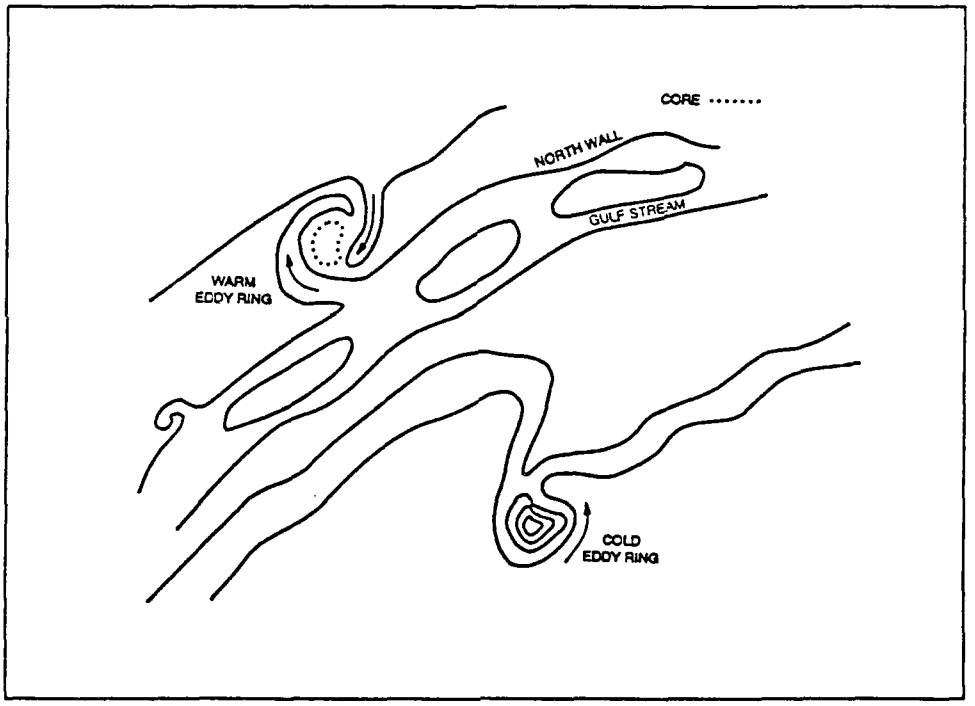

Figure 2. Contours (Isotherms)

Transformation to symbolic format is accomplished by performing a raster search to find at least one point on an edge contour (image isotherm). From this one point, a typical contour-following algorithm collects contiguous pixels into a list and eliminates or marks their extraction from the edge image. The raster search continues until all pixels are extracted.

The resulting collected lists contain numerous short isotherms such as those formed about cloud noise and "loose ends" left from the raster-scanning transformation process. Currently, OSIRRUS uses a rule that eliminates isotherms shorter than four points in length.

Clouds often leave streaks through otherwise uncontaminated thermal signature, breaking isotherms, and forming false termini of isotherms. A reconnection process ties isotherm termini together within a local neighborhood (without interpolating). The search process is on lists rather than contour following on the image, and is, therefore, an N^2 process where N equals number of isotherm termini. For a large number of termini, search becomes a compute intensive process. However, reconnection is not compute intensive since the original contour-following algorithm uses the same neighborhood to recursively trail and join isotherm termini. Reconnection, however, ensures unbroken isotherms and thus preserves whole shapes.

Finally, all collected isotherms are filtered a second time for length greater than or equal to 18 points. Generally, short isotherms will not embody enough shape to be recognized by the remaining detection scheme. Should additional algorithms be developed, groups of short isotherms (with adjacency) may be useful to detect partially occluded features. However, for the present time, this rule serves as a dividing line and data reduction limit.

2.3 Eddy-Shape Detection

Once isotherms are acquired in a symbolic format, shape recognition may begin. Eddy rings apparently have two major isotherm shape structures. The first of these structures is due to a turbulent swirling and mixing of cold and warmer waters. In such a case, isotherms tend to form a crested spiral or hook shape. During the development of OSIRRUS, a hook shape detector was developed and tested. However, simple schemes of hook and spiral detection failed to produce robust results. The reason for difficulty is probably that there are many subclasses of hook and spiral shapes. For example, warm eddy rings near the Gulf Stream pull colder slope water around from one side while pulling warmer water from near the north wall to the other side (see Figure 2). The shifting of waters in such fashion often creates apparent irregularities in the sensed gradient field.

The second major structure occurs when eddy rings no longer pull neighboring waters into shallow spirals. In this case, the core appears homogeneous and thermal gradients converge (or diverge) evenly from the ring center. One expects that isotherms would form concentric contours about the eddy ring. In general, the second structure is typified by concentric

open-ended bottles containing the eddy ring (see Figure 3). Currently, OSIRRUS uses only a bottle shape detector to filter isotherms with this type of major structure.

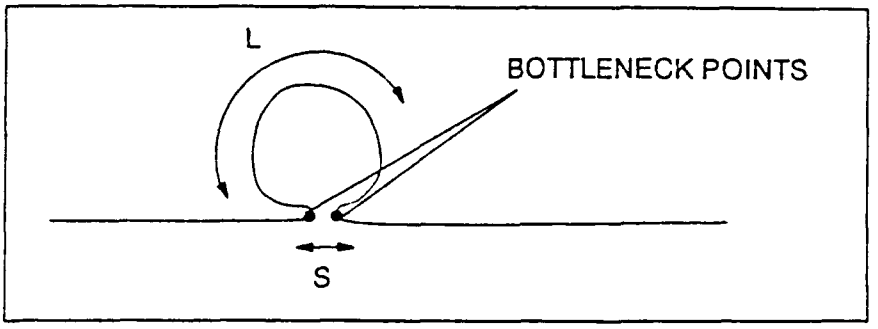

Figure 3. Bottleneck Filter

Currently, OSIRRUS employs an algorithm similar to a hill-climbing procedure which is faster than N^2 search. The algorithm finds the closest points (with euclidean separation S) that have at least a minimum arc length, L, between them. The two closest points generally mark the "neck" of the bottle or isotherm structure. Points between these bottleneck points are retained if local curvature is less than some threshold, $S/L < C_{Th}$. Thresholds governing the hill-climbing search serve as rules for detection.

Eddy rings are not always blessed with circular or ellipsoidal symmetry. Another filter involved in detection eliminates "bottles" that are considered extremely eccentric. The "ring filter" rule decides if a bottle-shaped isotherm is a possible component of an eddy ring:

$$(Rmax - Rmin)/RMS < \varepsilon \qquad (2)$$

where Rmax (Rmin) is the maximum (minimum) distance from the centroid of the bottle and RMS is the root-mean-square of all radii from the controid of the bottle. Epsilon is proportional to the maximum allowable eccentricity of the bottle.

Once bottles have been detected at all intensity (thermal) levels, OSIRRUS performs a grouping of concentric isotherms to strengthen or rank detection. Observations have indicated that centroids of isotherms about an eddy ring are not co-located. Therefore, bottles are grouped if within a neighborhood of radius = 16. Each group is then considered as one detection for analysis. A summary of detection rules is in Table II.

TABLE II
OSIRRUS DETECTION RULES

ISOTHERM FILTER	– MINIMUM ISOTHERM LENGTH (1ST) = 4 – MINIMUM ISOTHERM LENGTH (2ND) = 18
BOTTLENECK FILTER	– MAXIMUM BOTTLE SIZE = 80 – MAXIMUM NECKSIZE = 16 – MINIMUM BOTTLE LENGTH = 32 – MAXIMUM BOTTLE LENGTH = 256
RING FILTER	– (Rmax-Rmin)/RMS < .75
GROUPING	– R GROUP < 16

2.4 Feature Modeling

Feature modeling labels each detection with associated feature measurements which may: (a) help eliminate false detections; and (b) be of interest to an analyst reviewing the automatic interpretation. The feature suite is listed in Table III. The features are calculated by OSIRRUS from the grouped isotherms for each detection. Features form a structural list that represent an individual detection. The last feature, thermal profile, consists of 59 temperature-related measurements and is a temporary addition to the feature suite. The thermal profile feature is discussed in detail in Section 4.2.

A multiple discriminant analysis program called GOPAD has been used to determine the manner in which features can be combined to form identification rules.[1] GOPAD processed features of each detection together with groundtruth (i.e., known eddy rings). The result is a statistical model from a database of 117 images that provide distinguishability of actual eddy rings from false alarms. The effort to perform a statistical analysis was provided under extension of the OSIRRUS contract and is discussed at length in Section 4.0.

[1] Goal Oriented Pattern Detection, ThinkNet, Inc.

TABLE III
FEATURE ASSIGNMENT FOR EACH
EDDY RING DETECTION
(ISOTHERM GROUP)

- CENTROID X, Y
- MAXIMUM ISOTHERM LENGTH
- MINIMUM ISOTHERM LENGTH
- MAXIMUM EPSILON (OVALNESS)
- MINIMUM EPSILON (OVALNESS)
- MAXIMUM RADIUS
- MINIMUM RADIUS
- NUMBER OF ISOTHERMS IN GROUP
- THERMAL PROFILE (59 PARAMETERS)

2.5 Detection Results

Table IV shows results of detection prior to feature modeling. The table refers to results before and after optimizations and fine-tuning of rules, thresholds, etc., had been implemented. Four images are warmest-pixel composite (designated with an A---), and six are single images (designated with an M---). When comparing results, there are indications that combined results over a few days would be better than processing composite images where isotherms apparently broaden and smear.

These results have high false alarm rates since, to date, rules and methods have not been employed to eliminate detections due to noise. Many detections are too small to be eddy rings or have inconsistent thermal signature. The continuing effort to find elimination rules from a database of 100 images should bring false alarm rates down significantly.

TABLE IV
RESULTS SHOWING BEFORE AND AFTER OPTIMIZATION
AND IMPROVEMENT OF ALGORITHMS

IMAGE NAME	BEFORE A	D	F	M	E	AFTER A	D	F	M	E
A1T2	2	5	3	0		2	17	15	0	
A6Y7	1	5	4	0		1	11	10	0	
A17T18	2	5	4	1		2	7	5	0	
A21T23	1	6	6	1	clouds	1	15	15	1	
M09	3	4	3	2	clouds	3	18	17	2	clouds
M10B	4	6	4	2		4	15	11	0	
M10D	4	6	3	1		4	11	7	0	
M11A	4	7	5	2	clouds	4	11	8	1	clouds
M11C	3	5	2	0		3	11	8	4	
M12	1	8	7	0		1	13	12	0	
	25	57	41	9		25	129	108	4	

HITS= D-F=16
POD= HITS/ACTUAL=64%
FAR= F/D=72%

HITS= D-F=21
POD= HITS/ACTUAL=84%
FAR=F/D=84%

LEGEND
A - ACTUAL
D - DETECTED
F - FALSE ALARM
M - MISS
E - POSSIBLE REASON FOR MISSES
POD - PROBABILITY OF DETECTION
FAR - FALSE ALARM RATE

3.0 IMPROVEMENTS

Processing each intensity level to acquire isotherms is very time consuming. Yet, peculiar eddy rings may have domains over most of the 256 intensity levels. In order not to skip over possible detections and at the same time expedite processing, techniques were devised to process all intensity levels while clarifying information content that led to two major improvements in the speed of obtaining isotherms and improving isotherm representation for better eddy ring detection.

3.1 Modulation

The first technique may improve use of symbolic contours for many applications other than eddy ring detection. The process of "Image Modulation" for isotherm contour processing is based upon the following premise: "If the image topology is smooth and there are very few strong gradients over a base distance, B, then isotherms at a thresholding of t_1 are spatially separated from isotherms at a thresholding of $t_2 = t_1 + B$ at distances most like B." Thus, if B is large enough, the two isotherms at t_1 and at t_2 are almost always spatially separated. This separation allows the processing of more than one thresholding of an image at once without the

usual problems of adjacent and overlapping contours (isotherms). A pixel of intensity I(x,y) becomes:

$$I(X,Y) = MOD_B [I(X,Y)] + 1 \qquad (3)$$

where B is the base. After this modulation has been accomplished, B levels may be processed instead of 256! In order to ensure that the image is smooth, a specialized binomial filter is applied (see Section 3.2 below) before the modulation processing is completed.

Prior to implementing the image modulation scheme, the time to process ten levels of an image was 20 to 40 minutes. Thus, the expected time to process all 256 levels was about 8 to 17 hours. After implementation, images have been processed in full range (all 256 levels or 12 modulated levels) within an hour. Using this powerful approach, eddy rings are detected (both warm and cold rings), regardless of their internal or background temperature. Combined with other optimizations (not discussed herein), OSIRRUS currently can process 48 modulated levels in 15 minutes.

3.2 Special Gaussian

The second technique is required for the image modulation and further reduces noise and data representation. The method begins with a Gaussian filter (binomial 5x5) and normalizes the sum of weights corresponding to non-zero pixels. Using only non-zero pixels prevents cloud contaminated areas from becoming too smooth (like eddy rings) or blending with neighboring features. Isotherm representation is benefited because isotherms are smoother and represented with fewer points. Finally, isotherms are well separated before symbolic transformation takes place, resulting in less ambiguous shapes.

4.0 STATISTICAL ANALYSIS

The preliminary results discussed above have high false alarm rates since, to date, OSIRRUS has not employed rules and methods to eliminate false detections. Many detections are too small to be eddy rings or have inconsistent thermal signature. Further research was performed using a multiple discriminant analysis program called GOPAD to determine the manner in which features can be combined to form identification rules. GOPAD processed features of 1,107 detections together with ground truth (i.e., known eddy rings) resulting in two statistical models. The detections and associated features were obtained by using OSIRRUS to process a database of 117 images. Each model (one for warm eddy rings and one for cold eddy rings) provides a probability rule to distinguish actual eddy rings from false alarms.

4.1 OSIRRUS Results

The results of using OSIRRUS to process 117 256x256 images are presented below. Misses are considered to be any eddy rings unobscured and recognizable, correlating to charted analysis as groundtruth that were not detected by OSIRRUS. Eddy rings only partially in the image or more than 50% obscured by clouds are not considered detectable. The false alarms are those detections not eliminated by OSIRRUS and not correlating with groundtruth. The raw OSIRRUS results are in Table V.

TABLE V
RAW OSIRRUS RESULTS

ALL EDDY RINGS

ACTUAL \ OSIRRUS	ER	NOT	TTL
ER	87	42	129
NOT	1020	X	X
TTL	1107	X	X

FAR = 92.1% POD = 67.4%

WARM EDDY RINGS

ACTUAL \ OSIRRUS	ER	NOT	TTL
ER	30	26	56
NOT	581	X	X
TTL	611	X	X

FAR = 95.0% POD = 53.6%

COLD EDDY RINGS

ACTUAL \ OSIRRUS	ER	NOT	TTL
ER	57	16	73
NOT	439	X	X
TTL	496	X	X

FAR = 88.5% POD = 78.1%

LEGEND: ER = eddy rings; NOT = not eddy rings, TTL = total
FAR = False Alarm Rate
POD = Probability of Detection

These results reflect the ability of OSIRRUS to identify sets of concentric isotherms using only the bottle shape detector. Other shape detectors should increase the total number of hits and consequently reduce the number of misses for both cold and warm eddy rings.

4.2 Potential Predictor Variables (PPVs)

The potential predictor variables (PPVs) represent a set of measurements made for each detection that are to be used by GOPAD to establish a prediction model. The prediction model may then be used to provide the probability that a given detection is an eddy ring. The feature suite listed in Table III corresponds to the PPVs used to train GOPAD. The first nine PPVs provide location, shape and concentration of isotherms making up the detection. The next 59 PPVs provide a thermal profile of the detection.

The thermal profile PPVs are temperature-related measurements in the vicinity of the detection. Technically, these measurements are features (discussed in Section 2.4) and have been temporarily computed for the sake of the GOPAD statistical analysis. Assuming the detection is an eddy ring entirely enclosed by the maximum radius (RMAX) and that the eddy ring is approximately circular, regions of the image about the centroid are partitioned for measurement (see Figure 4). The CORE is arbitrarily defined as the inner circular area with radius half RMAX. The gradient region (GRD) is defined as an annulus between the core and radius RMAX, and the environment region (ENV) is defined as an annulus from radius RMAX to three halves RMAX. While these divisions and assumptions may oversimplify the actual thermal structure of eddy rings, they provide a consistent basis upon which to make comparisons. Each circular region is further partitioned into eight subregions. For each subregion, the mean temperature (intensity) and temperature variance is calculated to provide a total of 48 of the 59 thermal profile PPVs. By combining opposing core subregions, four core temperature slopes and four associated standard deviations may be calculated to provide eight more thermal profile PPVs. An additional three variables are formed by summing the mean temperatures of each subregion together for each circular region.

Although imagery should be processed in a standard fashion for consistent results, for our experimentation, OSIRRUS occasionally processed images with 256 compliment intensity values (reverse fielded). For these cases, the measured temperature means and slopes were easily corrected. However, a boolian variable (the only one) was provided to take into account any possible bias introduced by OSIRRUS. Altogether, there are 69 PPVs that are provided to GOPAD (see Appendix A for PPV names).

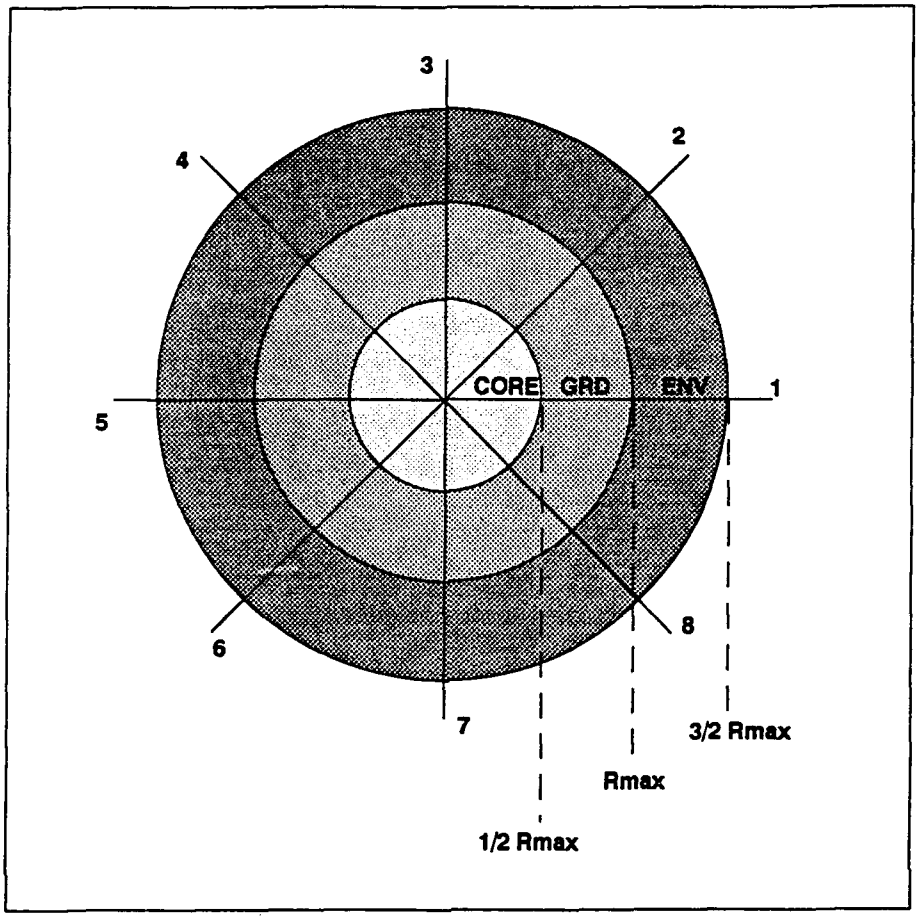

Figure 4. Thermal Profile of Eddy Ring

4.3 Semi-Automated Groundtruth Correlation

Using groundtruth charts (analyses) for imagery previously processed by OSIRRUS, a query program provided a semi-automated way of integrating groundtruth and OSIRRUS results, allowing for verification of integrated data. The query program begins by selecting an image from the database and displays the image on the screen and retrieves the corresponding OSIRRUS output for that image. The user is queried to process the image or skip to another image. If chosen, the query program asks if the image is reverse fielded and requests the x and y offsets. The program then displays detected eddy rings, with a Mercator grid overlaying the image showing latitude/longitude (lat/long) per grid line. The user may then mouse-click on each detected eddy ring corresponding to charted groundtruth. For each detection selected, lat/long values are displayed for verification of position. The user then specifies type (cold or warm) for the selection. After all detections are selected, the user terminates the selection loop

and all unselected detections are marked as false. The query program combines groundtruth information with the corresponding OSIRRUS output for that image and saves the resulting groundtruthed detections of all images in one file.

4.4 Data Preparation for GOPAD

After combining groundtruth with OSIRRUS detections using the query program, the data is formatted for GOPAD. Formatting the data included standardizing the PPVs for each detection and selecting groups of PPVs (indices) from which GOPAD will create optimized linear combinations. The indices selected are included in Appendix B. During the data preparation stage, detections were separated into a warm detections file and a cold detections file in order to create two independent prediction models. The method used to separate detections simply used the sign of the difference between the core and environment mean temperatures.

Standardization of a potential predictor variable is accomplished by computing the mean and standard deviation of that predictor variable value for all data points. The variable is then transformed by

$$X' = A*X+B \tag{4}$$

where

$$A = 1/\sigma \tag{5}$$

$$B = \bar{X}/\sigma. \tag{6}$$

4.5 GOPAD Results

GOPAD is a statistical analysis and modeling tool consisting of three major modules. The following paragraphs briefly describe the output from each module for both warm and cold models. The corresponding output data are listed in Appendices C, D, E, F, G, and H.

4.5.1 Module I

The first GOPAD module measures the statistical discriminatory ability of each individual predictor variable (including selected indices) to group detections in accordance with groundtruth. The value DSQ is a measure of separation between groups. After review of the set of predictor variables, GOPAD lists only those variables with a DSQ value greater than 5.00. Variables with values of DSQ less than 10.00 are not statistically significant as sole predictors

of groundtruth. However, all predictors listed with DSQ values are considered for inclusion in the model by the second GOPAD module.

The analysis conducted by the first GOPAD module clearly indicates the SHAPE index as having the highest discrimination ability in both warm and cold models. Although all variables combined to produce the SHAPE index have high DSQ values, the variable RMAX provides most of the discrimination. This result strongly suggests that the outermost contour detected (from a set of concentric contours combined using the bottle shape detector) must have a mean radius of sufficient size so that the contour contains or envelops an entire eddy ring. Also selected with high DSQ values were indices relating temperature variance, most significantly contributed by the core temperature variances. A high core variance may indicate a detection indicative of cloud cover, while a low core variance may indicate a smooth and near constant central temperature. Individually, the remaining predictor variables with low DSQ values are not good discriminators of eddy rings.

4.5.2 Module II

The second GOPAD module determines a near optimum combination of predictor variables from those provided from the first module. This module begins by creating combinations of two predictor variables and calculating respective DSQ values for each combination. Only the best pair of predictor variables is considered for further combination with a third predictor variable. The number of variables used in combination are increased until the improvement in DSQ is not statistically significant.

The warm model second module output selected only the SHAPE index (see Appendix B) in combination with the TCV3 predictor variable (variance of core temperature in the third octant), while the cold model second module output selected a combination of SHAPE and TENV (mean environment temperature in all octants) indices and the TCV8 and TCV6 predictor variables as having the best discriminatory power. These selected variables are passed on to the third GOPAD module.

4.5.3 Module III

The third module determines optimum scaling and orthogonalization of model predictor variables and determines optimal neighborhood size used in determining the probability that a given detection is an eddy ring. The orthogonalized predictor variables are given for each data

point and associated groundtruth. Module III provides a listing for each model predictor variable containing raw predictor variables, weights, and standardization coefficients. Also listed are the appropriate scale factors and eigenvectors for orthogonalization.

Reviewing the listings for both cold and warm models, one notices that only the first model predictor vector has non-zero values. This result indicates that all pertinent discriminatory information lies along a straight line in predictor variable space. Thus it is possible to establish a simple thresholding heuristic for discriminating actual eddy ring from false alarms. The prediction equations for both warm and cold models compute the magnitude of the first vector for a given detection, and are provided below.

PREDICTION EQUATIONS FOR COLD MODEL

PV1 = (0.5966E+00*RMAX) - (0.3618E-02*MINLEN) + (0.7114E+00*MAXEPSLN) + (0.5617E-02*NCTRS) + (0.2940E-02*TE4) - (0.2357E-02*TE6) + (0.2110E-06*TCV8) - (0.1860E-06*TCV6) - 0.1399E-01

PV2 = PV3 = PV4 = 0

PREDICTION EQUATIONS FOR WARM MODEL

PV1 = (0.6204E+00*RMAX) - (0.5938E+00*MAXLEN) - (0.3752E+00*MINEPSLN) - (0.2410E-06*TCV3) - (0.2269E+00)

PV2 = 0

4.6 Probability Forecast

Using the prediction equations above, it is possible to obtain a probability that a given detection is an eddy ring. The probability is generated from a K-Nearest-Neighbor algorithm. In general, the predictor vectors generated from a detection point to a place in predictor variable space from which K number of closest modeled data point neighbors (analogues) are referenced. The K neighbors will contain N actual eddy rings. The probability that the detection is an eddy ring is just P = N/K. GOPAD has determined the optimum number of neighbors used for both warm and cold models:

WARM MODEL	K = 22
COLD MODEL	K = 20

Therefore, using the appropriate prediction equation and modeled data points for a detection, a probability can be associated and indicated to the user. An interactive display could allow a threshold to be set, displaying only those detections above chosen probability.

4.7 Relative Operating Characteristics

Often, one desires to know the number of false alarms one must tolerate in order to retain a given percent of actual positive detections (eddy rings). Eliminating all false alarms may result in few positive detections, while retaining most positive detections could result in keeping most false alarms. A graph of false alarm rate verses percent detections reflects the relative operating characteristics for a particular model. The amount the curve deviates from the diagonal indicates the amount the prediction model may discriminate detections better than random chance. Figures 5 and 6 depict the relative operating characteristics for the warm and cold models.

5.0 CONCLUSIONS

OSIRRUS has proven the capability of symbolic processing to identify thermal structures for intelligent discrimination of eddy rings by shape recognition of image isotherms and by feature model identified regions. OSIRRUS can preprocess, transform image to list format, identify eddy shapes, and model extracted features in approximately 22 minutes per 256x256 image. In order to appreciate OSIRRUS' capability of shape recognition, one must consider that only one shape recognizer, the bottle filter, is employed. The results from processing 117 images show that this shape recognizer alone can achieve recognition of more than half of actual eddy rings presented. The overall performance of OSIRRUS on these images without any reduction of false alarms is as follows:

WARM EDDIES	53.6% POD	95.1% FAR
COLD EDDIES	78.1% POD	88.5% FAR
TOTAL EDDIES	67.4% POD	92.1% FAR

POD = Probability of Detection
FAR = False Alarm Rate

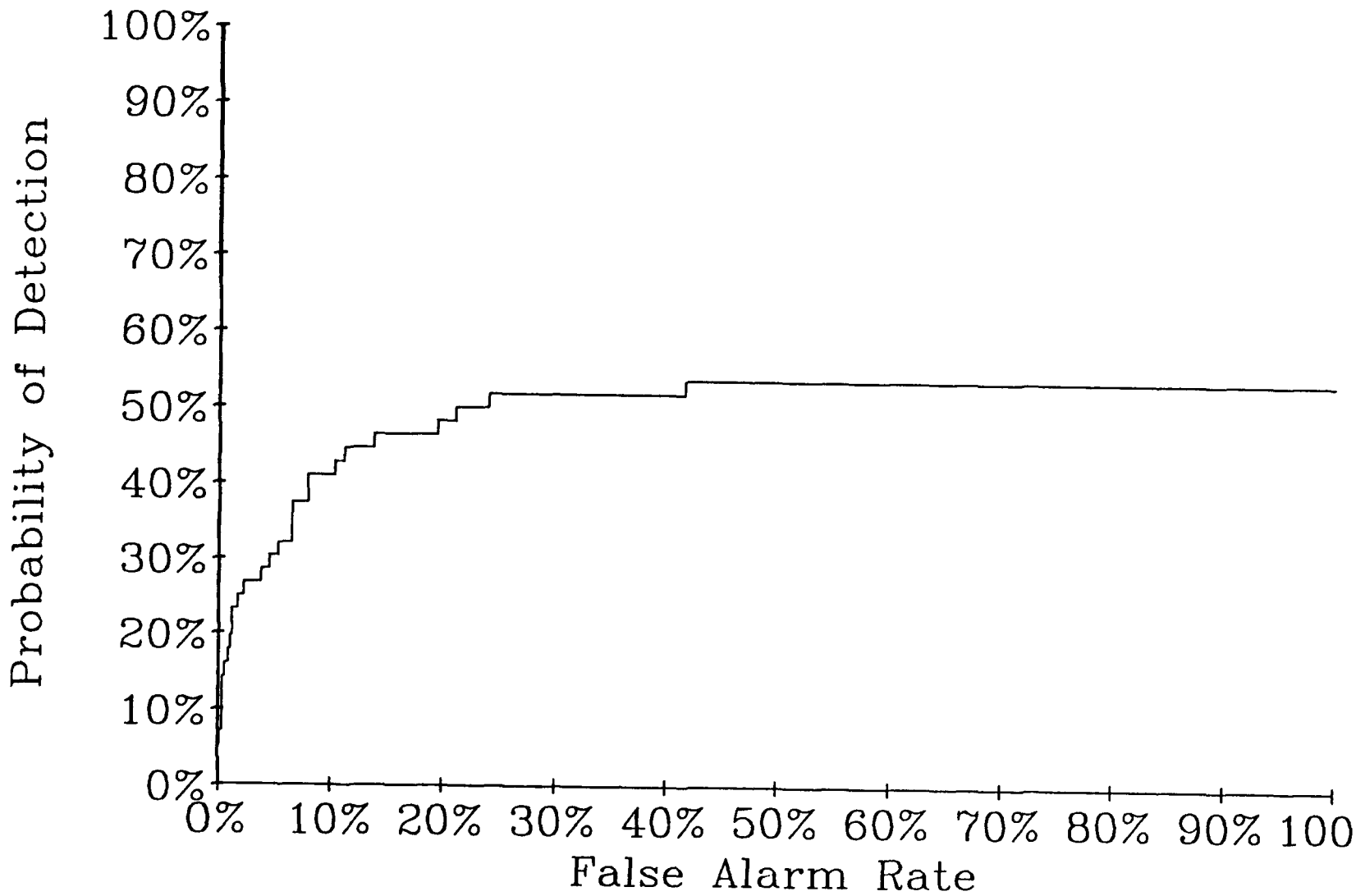

Figure 5. Warm Model Relative Operating Characteristics

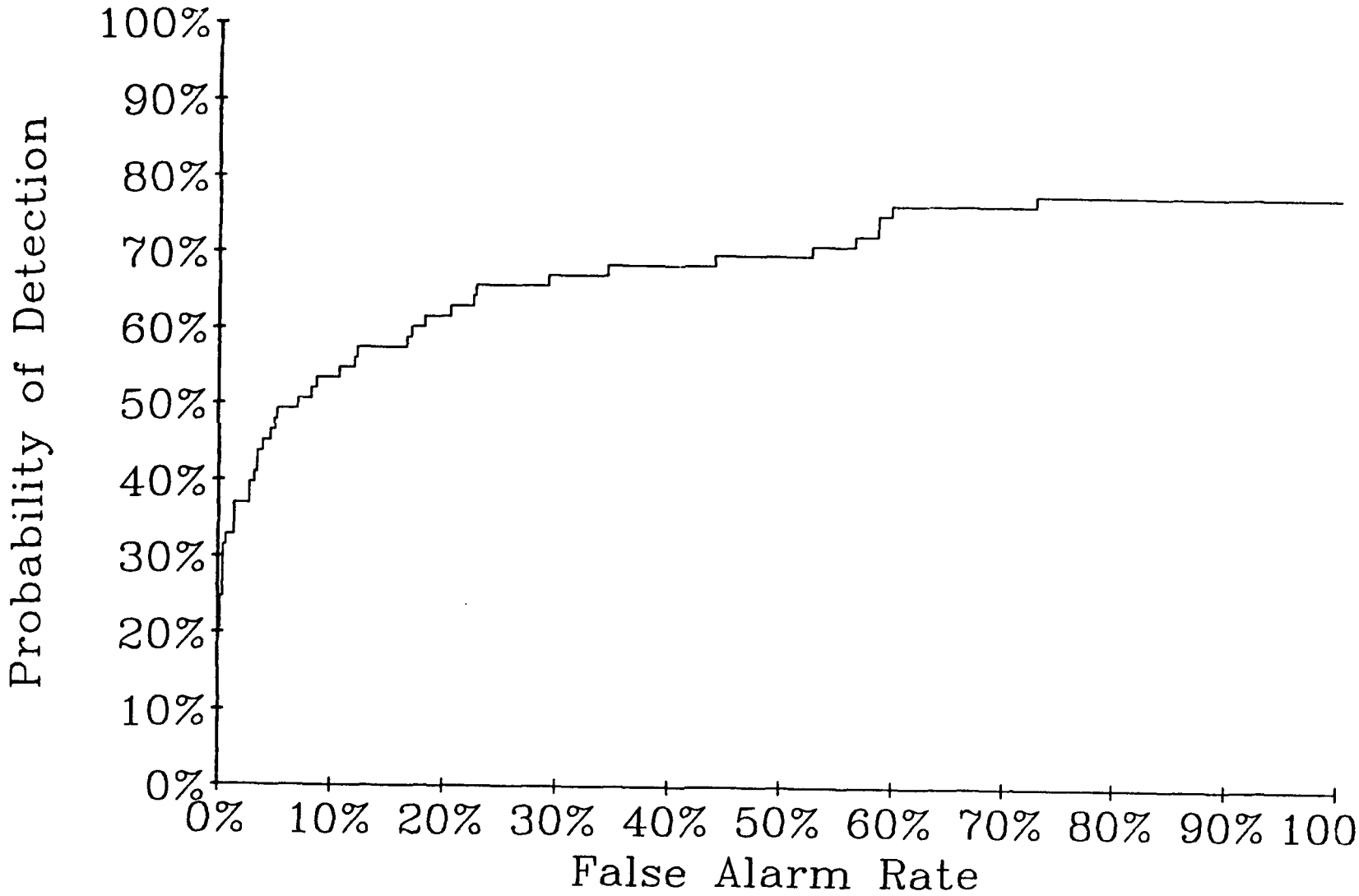

Figure 6. Cold Model Relative Operating Characteristics

A consequence of research in developing OSIRRUS is the implementation of special preprocessing of imagery by smoothing and Image Modulation to reduce processing time. The Image Modulation technique allows time-efficient, scale independent processing of all 256 intensity levels. Thus, OSIRRUS avoids submission to edge detection techniques that may be scale dependent. The acquisition of all isotherms in an image reduces the chance of loosing pertinent information. Furthermore, the transformation of imagery into isotherms as symbolic imagery provides for ease of efficient shape recognition and avoids mixed labeling of thermal structures.

Statistical analysis of detection-extracted features indicate that the overall size and shape is the most significant feature to discriminate false detections from actual eddy rings. Also there is some discriminate ability found in using the core temperature variance. Optimum prediction equations were established for both warm and cold detections. These equations and modeled data points allow a K-Nearest-Neighbor algorithm to calculate the eddy ring probability for a given detection. The probability could be displayed beside each circled detection for an analysts' review or thresholded for automatically deciding which detections are to be recorded in a database. Elimination of all but 10% of false alarms retains 53% of cold eddy rings and 42% of warm eddy rings. These results indicate that OSIRRUS is more likely to detect cold eddy rings than warm ones. This capability complements analysts who are prone to detect warm eddy rings more often than cold ones.

6.0 RECOMMENDATIONS

The above results were obtained from only one shape recognizer, the bottle filter. Continued research to create and test new shape recognizers would bring probability of detection to near 100% for eddy rings in the data provided. There are two possible shape recognizers that will detect characteristics of eddy ring thermal structure. One new shape detector would be a recreation of the previously developed hook detector. The hook detector developed early in the OSIRRUS project performed crudely and was abandoned for the more successful bottle shape detector. However, recreation of this filter would allow detections of spiral structured eddy rings. This structure is found in many of the warm eddy rings that pull cold slope water around in a fashion that causes an overall gradient across the warm ring. Another new shape detector would recognize adjacent isotherms with the proper curvature and thermal gradient as an eddy ring section (i.e., a pie slice). The pie filter would allow detection of partially obscured eddy rings from clouds or subduction by the Gulf Stream. These two new shape features (and possibly others) would provide independent detections of eddy rings, thereby increasing the

overall POD. For each shape filter, a groundtruth correlation and GOPAD analysis would be performed. Therefore, three shape detectors for warm and cold eddy rings would require six models. A seventh combined model, would provide a statistically sound basis for highest POD and lowest false alarm rate (FAR).

In order to achieve a more accurate statistical model using detection features, CCI recommends that a more refined database of detections be presented. Multiple detections result from differing image cuts (regions) of the same main image. Elimination of duplicate detections will result in a statistical model that is not biased from over emphasized features. CCI also recommends that detections correlated with groundtruth data be chosen to reflect the shape recognizers' intended function in order to eliminate coincidental hits from biasing the discriminatory ability of the statistical model.

Symbolic isotherm shape recognition may be extended to locate features within the Gulf Stream as an assist to temporal interpolation schemes. Thermal features currently not explored by NOARL can be extracted if characterized by shape, size, and thermal profile. Furthermore, CCI suggests that isotherm shape recognition has potential in the areas of image classification and image repair.

APPENDIX A

VARIABLE NAMES

Number	Name	Number	Name
1	MEANX	36	TGV3
2	MEANY	37	TGV4
3	MAXLEN	38	TGV5
4	MINLEN	39	TGV6
5	MAXEPSLN	40	TGV7
6	MINEPSLN	41	TGV8
7	RMAX	42	TC1
8	RMIN	43	TC2
9	NUMCTRS	44	TC3
10	TE1	45	TC4
11	TE2	46	TC5
12	TE3	47	TC6
13	TE4	48	TC7
14	TE5	49	TC8
15	TE6	50	TCV1
16	TE7	51	TCV2
17	TE8	52	TCV3
18	TEV1	53	TCV4
19	TEV2	54	TCV5
20	TEV3	55	TCV6
21	TEV4	56	TCV7
22	TEV5	57	TCV8
23	TEV6	58	TCM1
24	TEV7	59	TCM2
25	TEV8	60	TCM3
26	TG1	61	TCM4
27	TG2	62	TCMSTD1
28	TG3	63	TCMSTD2
29	TG4	64	TCMSTD3
30	TG5	65	TCMSTD4
31	TG6	66	REVP
32	TG7	67	TENV
33	TG8	68	TGRD
34	TGV1	69	TCORE
35	TGV2		

APPENDIX B
INDICES

```
  SHAPE     7
  (3   4    5    6    7    8    9)
   TEMP     3
 (67   68   69)
   TENV     8
 (10   11   12   13   14   15   16   17)
  TENVV     8
 (18   19   20   21   22   23   24   25)
   TGRD     8
 (26   27   28   29   30   31   32   33)
  TGRDV     8
 (34   35   36   37   38   39   40   41)
   TCOR     8
 (42   43   44   45   46   47   48   49)
  TCORV     8
 (50   51   52   53   54   55   56   57)
    TCM     4
 (58   59   60   61)
TCMSTD      4
 (62   63   64   65)
  TEGC0     3
 (10   26   42)
TEGCV0      3
 (18   34   50)
  TEGC1     3
 (11 27    43)
TEGCV1      3
 (19   35   51)
  TEGC2     3
 (12   28   44)
TEGCV2      3
 (20   36   52)
  TEGC3     3
 (13   29   45)
TEGCV3      3
 (21   37   53)
  TEGC4     3
 (14   30   4) 6
TEGCV4      3
 (22   38   54)
  TEGC5     3
 (15   31   47)
TEGCV5      3
 (23   39   55)
  TEGC6     3
 (16   32   48)
TEGCV6      3
 (24   40   56)
  TEGC7     3
 (17   33   49)
TEGCV7      3
 (25   41   57)
```

LEGEND:

1st Line: Index Name, #PVS
2nd Line: (List of PV #s)

APPENDIX C

WARM MODEL
MODULE I OUTPUT

SELECTED PREDICTOR VARIABLES

NAME	SEPARATION		LINEARITY
MAXLEN	DSQ =	133.17	0
MINLEN	DSQ =	73.21	0
MINEPSLN	DSQ =	16.73	0
RMAX	DSQ =	171.18	0
RMIN	DSQ =	100.48	0
NUMCTRS	DSQ =	25.19	0
TEV1	DSQ =	5.24	0
TCV1	DSQ =	117.65	0
TCV2	DSQ =	99.34	0
TCV3	DSQ =	145.16	0
TCV4	DSQ =	94.47	0
TCV5	DSQ =	132.91	0
TCV6	DSQ =	105.43	0
TCV7	DSQ =	108.79	0
TCV8	DSQ =	102.79	0

SELECTED PREDICTOR INDICES

NAME	SEPARATION	
SHAPE	DSQ =	225.41
TENVV	DSQ =	9.55
TEGCV0	DSQ =	125.23
TEGCV5	DSQ =	109.18

APPENDIX D

WARM MODEL
MODULE II OUTPUT

```
SELECTED VARIABLES  SHAPE
Overall   DSQ is   225.41
MAXLEN    DSQ =    224.70   0  Delta =    -0.71
MINLEN    DSQ =    225.41   0  Delta =     0.00
MINEPSLN  DSQ =    224.71   0  Delta =    -0.70
RMAX      DSQ =    224.69   0  Delta =    -0.72
RMIN      DSQ =    224.81   0  Delta =    -0.60
NUMCTRS   DSQ =    228.30   0  Delta =     2.89 BEST
TEV1      DSQ =    230.53   0  Delta =     5.12 BEST
TCV1      DSQ =    230.35   0  Delta =     4.94
TTCV2     DSQ =    225.25   0  Delta =    -0.16
TCV3      DSQ =    238.64   0  Delta =    13.23 BEST
TCV4      DSQ =    226.39   0  Delta =     0.98
TCV5      DSQ =    235.83   0  Delta =    10.42
TCV6      DSQ =    226.29   0  Delta =     0.88
TCV7      DSQ =    227.56   0  Delta =     2.15
TCV8      DSQ =    226.70   0  Delta =     1.29
TENVV     DSQ =    229.27   0  Delta =     3.86
TEGCV0    DSQ =    234.18   0  Delta =     8.77
TEGCV5    DSQ =    226.52   0  Delta =     1.11

SELECTED VARIABLES  SHAPE  TCV3
Overall   DSQ is   238.64
NUMCTRS   DSQ =    243.61   0  Delta =     4.96 BEST
TEV1      DSQ =    244.67   0  Delta =     6.03 BEST
TCV1      DSQ =    239.77   0  Delta =     1.13
TCV5      DSQ =    237.85   0  Delta =    -0.79
TENVV     DSQ =    243.18   0  Delta =     4.54
TEGCV0    DSQ =    237.90   0  Delta =    -0.74
```

APPENDIX E

WARM EDDY MODEL

```
NUMBER OF MODEL PREDICTOR VARIABLES   2
NUMBER OF DATA POINTS  611
NUMBER OF NEIGHBORS  22
FIRST MODEL PREDICTOR VARIABLE
NAME SHAPE
COMBINED FROM 3 PREDICTOR VARIABLES
     NAME       WEIGHT          A              B
     RMAX        1.00  0.90465978E-01 -0.87163365E+00
     MAXLEN     -0.60  0.14433134E-01 -0.84933436E+00
     MINEPSLN   -0.35  0.15631469E+01 -0.98760617E+00
SECOND MODEL PREDICTOR VARIABLE
NAME TCV3
COMBINED FROM 1 PREDICTOR VARIABLES
     NAME       WEIGHT          A              B
     TCV3        1.00  0.42875152E-06  0.22322698E+00
DIMENSIONAL SCALE FACTORS
 0.10000000E+01  0.00000000E+00
EIGENVECTORS
     VECTOR1         VECTOR2
 0.68588500E+01  0.36706083E+01
-0.51472348E+00  0.89091492E+00

MODELED DATA POINTS
NAME      GNDTH  VEC1     VEC2
JN0101     1.00 -0.641    0.000
JN0121     1.00 -0.272    0.000
JN0122     1.00 -0.208    0.000
JN0123     1.00 -0.775    0.000
JN0124     1.00 -0.043    0.000
JN0125     1.00  0.407    0.000
JN0145     1.00  1.105    0.000
JN0168     1.00 -0.531    0.000
JL0401     1.00 -1.271    0.000
JL0405     1.00 -0.996    0.000
JL0406     1.00 -0.420    0.000
JL0408     1.00  0.031    0.000
JL04011    1.00 -1.422    0.000
JN06I1     1.00 -0.853    0.000
JN06I2     1.00  0.593    0.000
JN06I4     1.00 -1.245    0.000
JN06I8     1.00 -0.695    0.000
JN06I9     1.00 -0.539    0.000
MY0542     1.00 -0.518    0.000
MY0543     2.00  7.810    0.000
MY0544     1.00 -0.930    0.000
MY0545     1.00 -0.849    0.000
MY0546     1.00  0.448    0.000
MY0547     1.00 -0.462    0.000
MY0549     1.00 -0.133    0.000
```

JL0601	1.00	0.037	0.000
JL0602	1.00	-0.403	0.000
JL0603	1.00	-0.972	0.000
JL0604	1.00	2.135	0.000
JL0621	1.00	-0.416	0.000
JL0622	1.00	-0.489	0.000
JL0623	1.00	-1.160	0.000
JL0627	1.00	-0.581	0.000
JL0628	1.00	-0.793	0.000
JL0629	1.00	-0.150	0.000
JL06211	1.00	2.191	0.000
JN0601	1.00	-0.873	0.000
JN0604	1.00	-0.113	0.000
JN0606	1.00	-1.004	0.000
JN0607	1.00	-1.398	0.000
JN06E1	1.00	0.187	0.000
JN06E3	1.00	-0.540	0.000
JN06E4	1.00	-0.579	0.000
JN06E5	1.00	-0.520	0.000
JN06E7	1.00	0.532	0.000
JN06G1	1.00	-1.237	0.000
JN06G5	1.00	0.593	0.000
DE0702	1.00	-0.672	0.000
DE0703	1.00	0.309	0.000
DE0704	1.00	-0.826	0.000
DE0707	1.00	-0.622	0.000
DE0721	1.00	-0.560	0.000
DE0722	1.00	1.735	0.000
DE0723	1.00	-1.016	0.000
DE0724	1.00	-2.214	0.000
DE0725	1.00	-1.127	0.000
DE0726	1.00	-2.357	0.000
DE0727	1.00	1.240	0.000
DE0729	1.00	-0.887	0.000
DE07211	1.00	2.938	0.000
AG0802	1.00	-0.511	0.000
AG0803	1.00	-0.891	0.000
AG0804	1.00	-0.528	0.000
AG0805	2.00	1.392	0.000
AG0806	1.00	1.225	0.000
AG0808	1.00	0.453	0.000
AG08010	1.00	-0.375	0.000
AG0821	1.00	-0.796	0.000
AG0822	1.00	-1.563	0.000
AG0825	1.00	-1.008	0.000
AG0826	1.00	0.459	0.000
AG0828	1.00	-0.511	0.000
AG0829	1.00	0.813	0.000
AG08211	1.00	-0.686	0.000
AG08212	1.00	-0.862	0.000
DE0802	2.00	3.300	0.000
DE0804	1.00	1.752	0.000
DE0821	1.00	-0.869	0.000
DE0825	1.00	1.752	0.000

DE0826	1.00	0.321	0.000
MY1142	1.00	-0.389	0.000
MY1143	1.00	-0.552	0.000
MY1144	1.00	-1.088	0.000
MY1145	1.00	0.732	0.000
MY1147	1.00	0.795	0.000
MY1149	1.00	-0.138	0.000
MY11410	2.00	1.811	0.000
MY11411	2.00	2.496	0.000
MY1162	2.00	1.618	0.000
MY1164	2.00	0.732	0.000
MY1166	1.00	-0.614	0.000
MY1167	1.00	-0.810	0.000
MY1168	1.00	-0.830	0.000
MY11610	1.00	0.547	0.000
JN0803	1.00	-0.298	0.000
JN0805	2.00	0.229	0.000
JN0807	1.00	0.024	0.000
JN0822	1.00	0.282	0.000
JN0823	1.00	4.225	0.000
JN0824	1.00	-0.982	0.000
JN0825	1.00	-0.721	0.000
JN0826	1.00	-0.292	0.000
JN0828	2.00	7.439	0.000
JN0842	1.00	-0.882	0.000
JN0843	1.00	-0.384	0.000
JN0844	1.00	-0.573	0.000
JN0845	1.00	0.338	0.000
JN0847	1.00	2.151	0.000
JN0849	1.00	-1.422	0.000
JN08411	2.00	4.749	0.000
JN0863	1.00	-1.366	0.000
JN0864	1.00	-0.650	0.000
JN0865	1.00	0.322	0.000
JN0866	1.00	-0.626	0.000
JN0868	1.00	0.696	0.000
JN08610	1.00	3.013	0.000
JN08612	1.00	-1.422	0.000
JN08613	1.00	-1.269	0.000
JN08616	1.00	0.169	0.000
JN08617	1.00	-0.214	0.000
JN08618	1.00	1.186	0.000
AG1003	1.00	-1.174	0.000
MY1102	1.00	0.318	0.000
MY1106	1.00	0.092	0.000
MY1121	1.00	-0.662	0.000
MY1122	1.00	-0.549	0.000
JN1241	1.00	-0.789	0.000
JN1242	1.00	0.392	0.000
JN1243	1.00	0.069	0.000
JN1244	1.00	1.935	0.000
JN1245	1.00	-0.555	0.000
JN1246	1.00	-0.854	0.000
JN1247	1.00	0.306	0.000

JN1248	1.00	-1.005	0.000
JN12410	1.00	-0.956	0.000
MY1102	1.00	-1.174	0.000
MY1103	1.00	-0.794	0.000
MY1106	1.00	-0.758	0.000
MY1108	1.00	0.509	0.000
MY1109	1.00	-0.086	0.000
MY11010	1.00	-0.075	0.000
MY11011	1.00	-1.453	0.000
MY11012	1.00	-0.637	0.000
MY11013	1.00	-0.043	0.000
MY11014	1.00	1.261	0.000
MY1121	1.00	-1.113	0.000
MY1124	1.00	-1.303	0.000
MY1126	1.00	0.032	0.000
MY1127	2.00	10.130	0.000
MY1129	1.00	0.240	0.000
MY11210	1.00	-0.651	0.000
MY11211	1.00	-0.738	0.000
MY1141	1.00	-0.849	0.000
MY1143	1.00	-0.924	0.000
MY1144	1.00	-0.799	0.000
MY1166	1.00	-1.338	0.000
MY1167	1.00	-0.325	0.000
JN1201	1.00	0.568	0.000
JN13C2	1.00	0.955	0.000
JN13C5	1.00	-0.466	0.000
JN13C7	1.00	0.882	0.00J
JN13E1	1.00	-0.498	0.000
JN13E5	1.00	0.462	0.000
JN13E7	1.00	-0.306	0.000
JN13E8	1.00	0.341	0.000
JN13E9	1.00	3.430	0.000
JN13G1	1.00	-0.874	0.000
JN13G2	1.00	-0.291	0.000
JN13G3	1.00	-0.916	0.000
JN13G4	1.00	-1.787	0.000
JN13G5	1.00	0.098	0.000
JN13G6	1.00	1.533	0.000
JN1301	1.00	-0.388	0.000
JN1303	1.00	0.067	0.000
JN1304	2.00	5.199	0.000
JN1305	1.00	0.239	0.000
JN1321	1.00	1.627	0.000
JN1322	1.00	0.384	0.000
JN1323	1.00	-0.455	0.000
JN1324	1.00	-1.231	0.000
JN1326	1.00	0.359	0.000
JN1328	1.00	-0.479	0.000
JN13210	1.00	-0.921	0.000
JN1343	1.00	-1.618	0.000
JN1344	1.00	-1.422	0.000
JN1345	1.00	-1.211	0.000
JN1347	1.00	-0.455	0.000

JN13412	1.00	-0.977	0.000
JN13413	2.00	1.384	0.000
JN13416	1.00	-0.920	0.000
JN1361	1.00	-0.756	0.000
JN1362	1.00	-0.209	0.000
JN1363	1.00	0.501	0.000
JN1364	1.00	-1.181	0.000
JN1365	1.00	-1.050	0.000
JN1366	2.00	5.882	0.000
JN1367	1.00	0.067	0.000
JN1368	1.00	-0.409	0.000
JN1369	1.00	-1.689	0.000
JN13610	1.00	-0.787	0.000
JN13611	1.00	0.623	0.000
JN1381	1.00	-0.784	0.000
JN1382	1.00	0.359	0.000
JN1384	2.00	5.343	0.000
JN1385	1.00	-0.549	0.000
JN1387	1.00	-0.479	0.000
JN13A1	1.00	1.270	0.000
JN13A12	1.00	-0.977	0.000
NO1542	1.00	-0.579	0.000
NO1544	1.00	1.046	0.000
NO1546	1.00	-0.544	0.000
NO1547	1.00	-0.761	0.000
NO1549	1.00	0.800	0.000
NO1562	1.00	0.343	0.000
NO1563	1.00	1.412	0.000
NO1564	1.00	1.046	0.000
NO1565	1.00	-0.039	0.000
NO1567	1.00	-1.014	0.000
NO1568	1.00	1.468	0.000
OC1601	1.00	-0.053	0.000
OC1603	1.00	-1.930	0.000
OC1605	1.00	-2.055	0.000
OC1607	1.00	-2.164	0.000
JN13I1	1.00	0.205	0.000
JN13I3	1.00	-0.034	0.000
JN13I4	1.00	0.290	0.000
JN13I9	1.00	-0.931	0.000
JN13I10	1.00	-0.016	0.000
JN13I11	1.00	-1.257	0.000
NO1402	1.00	-0.257	0.000
NO1404	1.00	0.197	0.000
NO1421	1.00	-0.607	0.000
NO1423	1.00	0.626	0.000
NO1426	1.00	0.393	0.000
NO1521	1.00	0.014	0.000
NO1522	1.00	0.128	0.000
NO1527	1.00	0.797	0.000
JL2301	1.00	-1.041	0.000
JL2302	1.00	-0.761	0.000
JL2303	1.00	-0.188	0.000
JL2305	1.00	0.604	0.000

JL2307	1.00	-1.026	0.000
JL2308	1.00	-1.636	0.000
JL2309	1.00	1.963	0.000
JL2321	1.00	1.398	0.000
JL2324	1.00	-0.838	0.000
JL2325	1.00	-1.000	0.000
JL2327	1.00	0.604	0.000
MY2402	1.00	0.622	0.000
MY2407	1.00	-0.587	0.000
MY2409	1.00	-1.166	0.000
MY24010	1.00	-0.925	0.000
MY2421	1.00	-0.879	0.000
MY2422	1.00	-0.650	0.000
MY2423	1.00	-0.468	0.000
MY2427	1.00	-0.627	0.000
MY2428	1.00	-0.702	0.000
MY24210	1.00	-1.294	0.000
MY24211	1.00	-1.098	0.000
MY24212	1.00	-0.315	0.000
MY24214	1.00	-1.184	0.000
MY24218	1.00	-1.184	0.000
MY24220	1.00	-0.499	0.000
JL2101	1.00	-0.438	0.000
JL2103	1.00	-1.066	0.000
JL2104	1.00	-0.888	0.000
JL2105	1.00	-0.438	0.000
JL2121	1.00	-0.414	0.000
JL2122	1.00	-1.247	0.000
JL2126	1.00	-0.226	0.000
JL21210	1.00	-0.999	0.000
JL21212	1.00	0.160	0.000
JL2141	1.00	0.164	0.000
JL2144	1.00	0.374	0.000
JL2146	1.00	0.707	0.000
JL2147	1.00	-0.019	0.000
NO2621	1.00	0.191	0.000
NO2622	1.00	1.304	0.000
NO2624	1.00	1.425	0.000
NO2625	2.00	1.099	0.000
NO2641	1.00	0.890	0.000
NO2642	1.00	-0.794	0.000
SE2601	1.00	-0.020	0.000
SE2602	1.00	-0.606	0.000
SE2603	1.00	-0.272	0.000
SE2604	1.00	0.478	0.000
SE2607	1.00	-0.435	0.000
SE2608	1.00	0.021	0.000
SE2609	1.00	-0.531	0.000
SE26011	1.00	0.991	0.000
SE2621	1.00	-0.115	0.000
SE2622	1.00	-0.071	0.000
SE2623	1.00	1.312	0.000
SE2625	1.00	0.191	0.000
SE2626	1.00	-0.075	0.000

SE2628	1.00	0.095	0.000
SE26210	1.00	-0.392	0.000
SE26212	1.00	2.108	0.000
SE26213	1.00	-1.555	0.000
SE26214	1.00	-0.142	0.000
MY2442	1.00	-0.460	0.000
MY2445	1.00	-0.297	0.000
MY2446	1.00	-0.248	0.000
MY2447	1.00	-1.108	0.000
MY24411	1.00	-0.626	0.000
MY24413	1.00	-0.903	0.000
AP2601	2.00	1.555	0.000
AP2602	1.00	-0.436	0.000
AP2603	1.00	0.670	0.000
AP2604	1.00	-0.022	0.000
AP2605	1.00	0.603	0.000
AP2606	1.00	-1.100	0.000
AP2621	1.00	0.713	0.000
AP2622	1.00	-1.563	0.000
AP2623	2.00	1.555	0.000
AP2624	1.00	-0.077	0.000
AP2625	1.00	-0.850	0.000
AP2626	1.00	-1.156	0.000
AP2627	1.00	-0.910	0.000
AP2629	1.00	-1.100	0.000
NO2602	1.00	0.191	0.000
NO2605	1.00	0.890	0.000
JL3001	2.00	-0.306	0.000
JL3003	2.00	2.101	0.000
JL3004	1.00	-0.267	0.000
JL3005	1.00	-0.735	0.000
JL3007	1.00	0.995	0.000
JL3021	1.00	-0.675	0.000
JL3022	1.00	1.866	0.000
JL3023	2.00	0.345	0.000
JL3026	1.00	-1.020	0.000
JL3028	1.00	-0.837	0.000
JL3029	1.00	-1.563	0.000
JL30210	1.00	0.027	0.000
MY3001	1.00	-0.336	0.000
MY3002	1.00	-0.209	0.000
MY3005	1.00	-1.041	0.000
MY3021	1.00	-0.209	0.000
MY3022	1.00	0.756	0.000
MY3023	1.00	-0.929	0.000
MY3024	1.00	-0.772	0.000
MY3025	1.00	-1.041	0.000
MY30211	1.00	-0.358	0.000
SE2801	1.00	-1.005	0.000
SE2803	1.00	-2.028	0.000
SE2804	1.00	-2.474	0.000
SE2805	1.00	-0.421	0.000
SE2809	1.00	-0.094	0.000
SE28010	1.00	0.265	0.000

SE2823	1.00	-0.094	0.000
SE2824	1.00	-0.657	0.000
SE2842	1.00	-0.840	0.000
SE2843	1.00	-0.937	0.000
SE2844	1.00	-0.400	0.000
SE2845	1.00	0.085	0.000
JL3122	1.00	0.952	0.000
JN0111	1.00	-0.935	0.000
JN0112	1.00	-0.381	0.000
JN0113	1.00	-0.497	0.000
JN0118	1.00	-0.231	0.000
JN0132	1.00	0.168	0.000
JN0133	1.00	-1.466	0.000
JN0137	1.00	1.433	0.000
JN0138	1.00	0.898	0.000
JN01312	1.00	-0.497	0.000
JN01315	1.00	2.926	0.000
JN01H1	1.00	-1.181	0.000
JN01H2	1.00	-1.366	0.000
JN01H4	1.00	0.125	0.000
JN01H7	1.00	-0.948	0.000
JN01H8	1.00	-1.468	0.000
JN01H9	1.00	0.194	0.000
JN01H10	1.00	-1.664	0.000
JN01H11	1.00	-0.847	0.000
JN01H12	1.00	-1.622	0.000
JN01H14	1.00	0.263	0.000
MY3042	1.00	-0.015	0.000
MY3043	1.00	-1.772	0.000
MY3047	1.00	2.980	0.000
MY3049	1.00	-0.828	0.000
MY3063	1.00	-0.890	0.000
MY3064	1.00	-0.181	0.000
MY3066	1.00	0.022	0.000
JL3101	1.00	-0.442	0.000
JL3102	1.00	0.023	0.000
JL3103	1.00	-0.930	0.000
JL3104	1.00	-0.371	0.000
JL3105	1.00	-1.381	0.000
JL3106	1.00	0.528	0.000
JL3107	1.00	-1.399	0.000
JL3108	1.00	-1.119	0.000
JL3109	1.00	-0.816	0.000
JL31010	1.00	3.017	0.000
JL31011	1.00	-1.141	0.000
JL31012	1.00	0.239	0.000
JL31013	1.00	0.146	0.000
JL31014	1.00	-0.622	0.000
JL31016	1.00	0.176	0.000
MY1015	1.00	-0.146	0.000
MY1032	1.00	-1.444	0.000
MY1033	1.00	3.420	0.000
MY1035	1.00	-0.918	0.000
MY1037	1.00	-0.876	0.000

MY1039	1.00	-0.715	0.000
MY10311	1.00	-1.361	0.000
MY10313	1.00	-0.783	0.000
MY1051	1.00	-0.801	0.000
MY1052	1.00	-0.790	0.000
MY1053	1.00	0.119	0.000
MY1054	1.00	-0.715	0.000
MY1055	1.00	0.853	0.000
MY1058	1.00	-0.964	0.000
MY1073	1.00	-0.351	0.000
MY1074	1.00	-1.066	0.000
MY1076	1.00	0.853	0.000
JN1111	1.00	-1.524	0.000
JN1113	1.00	-1.739	0.000
JN1115	1.00	-1.307	0.000
JN1117	1.00	0.157	0.000
JN11110	1.00	-1.253	0.000
JN11111	1.00	0.715	0.000
JN11112	2.00	4.064	0.000
JN11113	1.00	-0.629	0.000
JN11115	1.00	4.295	0.000
JN11116	1.00	-0.549	0.000
JN1132	1.00	-0.496	0.000
JN1137	1.00	-0.728	0.000
JN11310	1.00	-1.861	0.000
JN01J1	1.00	-1.085	0.000
JN01J5	1.00	5.643	0.000
JN01J6	1.00	-1.416	0.000
JN01J7	1.00	-0.336	0.000
JN01J8	1.00	-0.927	0.000
JN01J9	1.00	-1.450	0.000
JN0915	1.00	-0.574	0.000
JN0919	1.00	1.778	0.000
JN09110	1.00	-1.576	0.000
JN09111	2.00	4.612	0.000
JN0931	1.00	-0.520	0.000
JN0932	1.00	-0.675	0.000
JN0933	1.00	-0.521	0.000
JN0934	1.00	-0.422	0.000
JN0935	1.00	-0.945	0.000
JN0936	1.00	-0.673	0.000
JN0939	1.00	-0.441	0.000
MY1111	1.00	-0.415	0.000
MY1112	1.00	-0.628	0.000
MY1113	1.00	4.077	0.000
MY1114	1.00	-1.127	0.000
MY1115	1.00	-0.177	0.000
MY1117	1.00	5.481	0.000
MY1119	1.00	0.815	0.000
MY11111	1.00	-0.381	0.000
MY1134	1.00	0.439	0.000
MY1135	1.00	-0.517	0.000
MY1136	2.00	0.973	0.000
MY1153	1.00	-0.178	0.000

MY1155	1.00	1.073	0.000
MY1157	1.00	2.531	0.000
MY1171	1.00	3.518	0.000
MY1178	1.00	-1.076	0.000
MY11711	1.00	-1.351	0.000
MY11712	1.00	-0.725	0.000
MY11715	1.00	-0.921	0.000
MY11716	1.00	-0.262	0.000
MY11F3	1.00	-1.067	0.000
MY11F4	1.00	0.099	0.000
MY11F5	2.00	6.141	0.000
MY11H2	1.00	-0.665	0.000
MY11H5	1.00	-0.205	0.000
MY11H7	1.00	-0.800	0.000
MY11H9	1.00	0.609	0.000
MY11H11	1.00	-1.239	0.000
MY11H12	1.00	0.046	0.000
MY11H13	1.00	1.261	0.000
JN1171	1.00	-1.049	0.000
JN1172	1.00	-1.524	0.000
JN1173	1.00	-1.535	0.000
JN1175	1.00	-1.631	0.000
JN1176	1.00	-0.693	0.000
JN1177	1.00	-1.463	0.000
JN1178	1.00	4.807	0.000
JN1179	1.00	-1.369	0.000
JN11710	1.00	-0.127	0.000
SE1611	1.00	-0.796	0.000
SE1615	1.00	0.105	0.000
SE1618	1.00	-1.881	0.000
SE1619	1.00	-1.649	0.000
SE16110	1.00	-0.811	0.000
SE1635	1.00	-0.585	0.000
SE1636	1.00	-0.076	0.000
SE1637	1.00	-1.114	0.000
SE1639	1.00	0.414	0.000
SE16312	1.00	0.037	0.000
SE16315	1.00	-0.301	0.000
JN3014	1.00	-1.457	0.000
JN3017	1.00	-1.566	0.000
JN3018	1.00	-1.314	0.000
JN3019	1.00	-0.160	0.000
JN30110	1.00	-0.367	0.000
JN30111	1.00	-1.135	0.000
JN3032	1.00	0.043	0.000
JN3033	1.00	-0.679	0.000
JN3034	1.00	-0.712	0.000
JN3037	1.00	-0.142	0.000
JN3038	1.00	-0.132	0.000
JN3052	1.00	-0.993	0.000
JN3053	1.00	-0.013	0.000
JN3054	2.00	5.625	0.000
JN3057	1.00	0.704	0.000
JN3071	1.00	-1.254	0.000

JN3072	1.00	0.454	0.000
JN3073	1.00	1.909	0.000
JN3074	1.00	-1.049	0.000
JN3075	1.00	1.334	0.000
JN3078	1.00	-0.821	0.000
JN3093	1.00	7.531	0.000
JN3095	1.00	-0.131	0.000
JN3097	1.00	-1.160	0.000
JN3098	1.00	-1.383	0.000
JN3099	1.00	1.349	0.000
JN30910	1.00	-1.018	0.000
JN30911	1.00	0.308	0.000
JN30913	1.00	-1.169	0.000
JN30914	1.00	-1.424	0.000
MY11J1	1.00	-0.693	0.000
MY11J3	1.00	0.037	0.000
MY11J5	1.00	-0.510	0.000
MY11J8	1.00	1.174	0.000
MY11L2	1.00	-0.792	0.000
MY11L4	1.00	-0.424	0.000
MY11L5	1.00	0.648	0.000
MY11L6	2.00	17.931	0.000
MY11L7	1.00	-0.686	0.000
MY11L9	1.00	-0.835	0.000
MY11L11	1.00	1.495	0.000
MY11L12	1.00	-0.046	0.000
JL0422	1.00	-1.070	0.000
JL0424	1.00	-0.149	0.000
JL0425	1.00	-0.926	0.000
JL0426	1.00	-0.888	0.000
JL0427	1.00	0.031	0.000
JL0429	2.00	0.436	0.000
JL04210	1.00	0.121	0.000
JL04212	1.00	-0.567	0.000
AP29E2	1.00	2.733	0.000
AP29E3	1.00	1.236	0.000
AP29E5	1.00	3.011	0.000
AP29E7	1.00	0.651	0.000
AP29E8	1.00	-0.881	0.000
AP29E10	1.00	-0.450	0.000
AP29E13	1.00	-0.078	0.000
AP29E15	1.00	5.204	0.000
AP29E17	1.00	1.435	0.000
JN1152	1.00	-1.631	0.000
JN1154	1.00	9.036	0.000
JN1157	1.00	-0.790	0.000
JN1158	2.00	9.947	0.000
JN01F1	1.00	5.367	0.000
JN01F4	1.00	-0.435	0.000
JN01F5	1.00	-1.064	0.000
JN01F6	1.00	-0.681	0.000
JN01F9	1.00	-0.998	0.000
JN01F10	1.00	1.937	0.000
AP2801	1.00	-1.243	0.000

AP2805	1.00	0.398	0.000
AP2807	1.00	-1.724	0.000
AP2808	1.00	-0.867	0.000
AP2809	1.00	-1.086	0.000
AP28010	1.00	-0.424	0.000
AP28011	1.00	1.661	0.000
AP28014	1.00	-0.978	0.000
AP28015	1.00	-0.565	0.000
AP28017	1.00	-0.394	0.000
AP28018	1.00	-0.576	0.000
AP28019	1.00	-0.803	0.000
AP28021	1.00	-1.376	0.000
AP28022	2.00	7.457	0.000
AP28024	1.00	-0.551	0.000
AP2301	1.00	-1.466	0.000
AP2302	1.00	1.303	0.000
AP2303	1.00	-0.712	0.000
AP2304	1.00	-0.677	0.000
AP2305	1.00	-1.114	0.000
AP2306	1.00	0.374	0.000
AP2308	1.00	-1.307	0.000
AP2309	1.00	-2.479	0.000
AP23010	1.00	0.575	0.000
AP23012	1.00	0.283	0.000
AP23014	1.00	-0.074	0.000
AP23016	1.00	-1.403	0.000
AP2203	1.00	2.892	0.000
AP2204	1.00	-0.486	0.000
AP2206	1.00	-1.285	0.000
JN1221	1.00	-1.053	0.000
JN1222	1.00	1.793	0.000
JN1223	1.00	-0.789	0.000
JN1224	1.00	-0.854	0.000
JN1225	1.00	0.069	0.000
JN1227	1.00	0.548	0.000
JN06I1	1.00	-0.853	0.000
JN06I2	1.00	0.593	0.000
JN06I4	1.00	-1.245	0.000
JN06I8	1.00	-0.695	0.000
JN06I9	1.00	-0.539	0.000
MY0523	1.00	-0.428	0.000
MY0524	1.00	0.095	0.000
MY0526	1.00	-1.307	0.000
MY0502	1.00	-1.270	0.000
MY0503	1.00	-0.800	0.000
MY0505	1.00	-1.300	0.000

NAME LEGEND:

MMDDCN(N)
M = Month
D = Day
C = Year & Type Code
N = Nth Image Detection

APPENDIX F

COLD MODEL
MODULE I OUTPUT

SELECTED PREDICTOR VARIABLES

NAME	SEPARATION		
MAXLEN	DSQ =	195.36	0
MINLEN	DSQ =	54.78	0
MINEPSLN	DSQ =	30.88	0
RMAX	DSQ =	228.58	0
RMIN	DSQ =	64.29	0
NUMCTRS	DSQ =	64.90	0
TE1	DSQ =	7.17	0
TE2	DSQ =	7.70	0
TE3	DSQ =	7.85	0
TE4	DSQ =	8.94	0
TE5	DSQ =	8.16	0
TE6	DSQ =	6.81	0
TE7	DSQ =	6.64	0
TE8	DSQ =	7.41	0
TEV1	DSQ =	6.64	0
TEV6	DSQ =	6.14	0
TG1	DSQ =	6.39	0
TG2	DSQ =	7.02	0
TG3	DSQ =	7.41	0
TG4	DSQ =	7.17	0
TG5	DSQ =	6.75	0
TG6	DSQ =	6.72	0
TG7	DSQ =	6.48	0
TG8	DSQ =	6.68	0
TC1	DSQ =	6.58	0
TC2	DSQ =	7.34	0
TC3	DSQ =	6.40	0
TC4	DSQ =	7.10	0
TC5	DSQ =	6.47	0
TC6	DSQ =	7.03	0
TC7	DSQ =	6.85	0
TC8	DSQ =	7.63	0
TCV1	DSQ =	104.48	0
TCV2	DSQ =	31.31	0
TCV3	DSQ =	106.57	0
TCV4	DSQ =	47.66	0
TCV5	DSQ =	110.47	0
TCV6	DSQ =	39.31	0
TCV7	DSQ =	107.97	0
TCV8	DSQ =	35.68	0
TCMSTD1	DSQ =	6.56	0
REVP	DSQ =	7.86	0
TENV	DSQ =	7.66	0
TGRD	DSQ =	6.86	0
TCORE	DSQ =	6.97	0

```
SELECTED PREDICTOR INDICES
NAME        SEPARATION
SHAPE    DSQ =    263.23
TENV     DSQ =     13.15
TCORV    DSQ =    123.04
TCMSTD   DSQ =     10.86
TEGCV4   DSQ =    114.74
TEGCV5   DSQ =     44.48
```

APPENDIX G

COLD MODEL
MODULE II OUTPUT

SELECTED VARIABLES	SHAPE				
Overall	DSQ is	263.23			
MAXLEN	DSQ =	262.67	0	Delta =	-0.56
MINLEN	DSQ =	263.00	0	Delta =	-0.23
MINEPSLN	DSQ =	264.94	0	Delta =	1.71
RMAX	DSQ =	262.82	0	Delta =	-0.41
RMIN	DSQ =	263.09	0	Delta =	-0.14
NUMCTRS	DSQ =	262.77	0	Delta =	-0.46
TE1	DSQ =	265.32	0	Delta =	2.09
TE2	DSQ =	265.48	0	Delta =	2.25
TE3	DSQ =	266.19	0	Delta =	2.96 BEST
TE4	DSQ =	266.73	0	Delta =	3.50 BEST
TE5	DSQ =	266.00	0	Delta =	2.77
TE6	DSQ =	265.07	0	Delta =	1.84
TE7	DSQ =	264.89	0	Delta =	1.66
TE8	DSQ =	265.55	0	Delta =	2.32
TEV1	DSQ =	266.16	0	Delta =	2.93
TEV6	DSQ =	265.05	0	Delta =	1.82
TG1	DSQ =	264.98	0	Delta =	1.75
TG2	DSQ =	265.10	0	Delta =	1.87
TG3	DSQ =	265.54	0	Delta =	2.31
TG4	DSQ =	265.42	0	Delta =	2.19
TG5	DSQ =	265.02	0	Delta =	1.79
TG6	DSQ =	265.21	0	Delta =	1.98
TG7	DSQ =	265.41	0	Delta =	2.18
TG8	DSQ =	265.01	0	Delta =	1.78
TC1	DSQ =	265.64	0	Delta =	2.41
TC2	DSQ =	264.86	0	Delta =	1.63
TC3	DSQ =	265.22	0	Delta =	1.99
TC4	DSQ =	264.78	0	Delta =	1.55
TC5	DSQ =	265.28	0	Delta =	2.05
TC6	DSQ =	265.21	0	Delta =	1.98
TC7	DSQ =	266.03	0	Delta =	2.80
TC8	DSQ =	265.36	0	Delta =	2.13
TCV1	DSQ =	262.30	0	Delta =	-0.93
TCV2	DSQ =	270.36	0	Delta =	7.13 BEST
TCV3	DSQ =	262.24	0	Delta =	-0.99
TCV4	DSQ =	265.83	0	Delta =	2.60
TCV5	DSQ =	265.96	0	Delta =	2.73
TCV6	DSQ =	267.56	0	Delta =	4.33
TCV7	DSQ =	262.26	0	Delta =	-0.97
TCV8	DSQ =	270.54	0	Delta =	7.31 BEST
TCMSTD1	DSQ =	264.58	0	Delta =	1.35
REVP	DSQ =	265.52	0	Delta =	2.29
TENV	DSQ =	265.67	0	Delta =	2.44
TGRD	DSQ =	265.22	0	Delta =	1.99
TCORE	DSQ =	265.31	0	Delta =	2.08

```
TENV      DSQ =   271.73  0  Delta =    8.50 BEST
TCORV     DSQ =   263.94  0  Delta =    0.71
TCMSTD    DSQ =   264.39  0  Delta =    1.16
TEGCV4    DSQ =   268.84  0  Delta =    5.61
TEGCV5    DSQ =   264.32  0  Delta =    1.09


SELECTED VARIABLES  SHAPE  TENV
Overall   DSQ is   271.73
TE3       DSQ =   271.50  0  Delta =   -0.23
TE4       DSQ =   271.63  0  Delta =   -0.10
TE5       DSQ =   271.72  0  Delta =   -0.01
TEV1      DSQ =   273.76  0  Delta =    2.03
TC1       DSQ =   271.57  0  Delta =   -0.16
TC7       DSQ =   271.21  0  Delta =   -0.52
TCV2      DSQ =   282.17  0  Delta =   10.44 BEST
TCV4      DSQ =   276.86  0  Delta =    5.13
TCV5      DSQ =   273.25  0  Delta =    1.52
TCV6      DSQ =   279.54  0  Delta =    7.81
TCV8      DSQ =   282.95  0  Delta =   11.22 BEST
TENV      DSQ =   271.75  0  Delta =    0.02
TEGCV4    DSQ =   275.25  0  Delta =    3.52

SELECTED VARIABLES  SHAPE  TENV  TCV8
Overall   DSQ is   282.95
TCV2      DSQ =   281.86  0  Delta =   -1.09
TCV4      DSQ =   295.65  0  Delta =   12.70 BEST
TCV6      DSQ =   295.89  0  Delta =   12.94 BEST
TEGCV4    DSQ =   289.47  0  Delta =    6.52

SELECTED VARIABLES  SHAPE  TENV  TCV8  TCV6
Overall   DSQ is   295.89
TCV4      DSQ =   297.42  0  Delta =    1.53
TEGCV4    DSQ =   294.94  0  Delta =   -0.95
```

APPENDIX H

COLD EDDY MODEL

```
NUMBER OF MODEL PREDICTOR VARIABLES   4
NUMBER OF DATA POINTS  496
NUMBER OF NEIGHBORS  20
FIRST MODEL PREDICTOR VARIABLE
NAME  SHAPE
COMBINED FROM 4 PREDICTOR VARIABLES
     NAME        WEIGHT          A           B
     RMAX         1.00  0.78082673E-01 -0.83893758E+00
     MINLEN      -0.30  0.15784204E-01 -0.85743874E+00
     MAXEPSLN    -0.65  0.14323337E+01 -0.99510837E+00
     NUMCTRS      0.10  0.73499016E-01 -0.36971784E+00
SECOND MODEL PREDICTOR VARIABLE
NAME  TENV
COMBINED FROM 2 PREDICTOR VARIABLES
     NAME        WEIGHT          A           B
     TE4          1.00  0.11317214E-01 -0.58443499E+00
     TE6         -0.80  0.11345428E-01 -0.59607500E+00
THIRD MODEL PREDICTOR VARIABLE
NAME  TCV8
COMBINED FROM 1 PREDICTOR VARIABLES
     NAME        WEIGHT          A           B
     TCV8         1.00  0.32789899E-06 -0.98725162E-01
FOURTH MODEL PREDICTOR VARIABLE
NAME  TCV6
COMBINED FROM 1 PREDICTOR VARIABLE
     NAME        WEIGHT          A           B
TCV6       1.00  0.32333392E-06 -0.96740544E-01
DIMENSIONAL SCALE FACTORS
 0.10000000E+01  0.00000000E+00  0.00000000E+00  0.00000000E+00
EIGENVECTORS
     VECTOR1         VECTOR2         VECTOR3         VECTOR4
 0.76423985E+00  0.11384188E+01  0.11384188E+01 -0.60486352E+00
 0.25971833E+00  0.18380252E+01  0.18380252E+01  0.13676803E+01
 0.64493215E+00  0.27418742E+01  0.27418742E+01 -0.12933538E+01
-0.57809085E+00 -0.11791501E+01 -0.11791501E+01  0.75909460E+00

MODELED DATA POINTS
NAME      GNDTH  VEC1    VEC2    VEC3    VEC4
JN0102     2.00  0.711   0.000   0.000   0.000
JN0103     1.00 -0.224   0.000   0.000   0.000
JN0141     1.00 -0.264   0.000   0.000   0.000
JN0142     1.00 -0.365   0.000   0.000   0.000
JN0143     2.00  0.529   0.000   0.000   0.000
JN0144     1.00 -0.271   0.000   0.000   0.000
JN0146     2.00  0.789   0.000   0.000   0.000
JN0147     1.00 -0.102   0.000   0.000   0.000
JN0161     1.00 -0.365   0.000   0.000   0.000
JN0162     2.00 -0.171   0.000   0.000   0.000
JN0163     1.00 -0.311   0.000   0.000   0.000
```

JN0164	1.00	-0.154	0.000	0.000	0.000
JN0165	1.00	-0.264	0.000	0.000	0.000
JN0166	1.00	-0.231	0.000	0.000	0.000
JN0167	2.00	0.378	0.000	0.000	0.000
JN0169	1.00	-0.052	0.000	0.000	0.000
JL0402	1.00	0.649	0.000	0.000	0.000
JL0403	1.00	0.244	0.000	0.000	0.000
JL0404	1.00	-0.082	0.000	0.000	0.000
JL0407	1.00	0.221	0.000	0.000	0.000
JL0409	1.00	-0.272	0.000	0.000	0.000
JL04010	1.00	-0.373	0.000	0.000	0.000
JN06I3	1.00	0.033	0.000	0.000	0.000
JN06I5	1.00	0.657	0.000	0.000	0.000
JN06I6	1.00	0.063	0.000	0.000	0.000
JN06I7	1.00	-0.080	0.000	0.000	0.000
JN06I10	1.00	-0.214	0.000	0.000	0.000
MY0541	1.00	-0.198	0.000	0.000	0.000
MY0548	1.00	0.427	0.000	0.000	0.000
JL0624	1.00	0.037	0.000	0.000	0.000
JL0625	1.00	-0.176	0.000	0.000	0.000
JL0626	1.00	0.028	0.000	0.000	0.000
JL06210	1.00	-0.036	0.000	0.000	0.000
JL06212	1.00	0.395	0.000	0.000	0.000
JL06213	1.00	-0.056	0.000	0.000	0.000
JL06214	1.00	0.076	0.000	0.000	0.000
JL06215	1.00	0.441	0.000	0.000	0.000
JN0602	1.00	-0.263	0.000	0.000	0.000
JN0603	1.00	-0.126	0.000	0.000	0.000
JN0605	1.00	-0.029	0.000	0.000	0.000
JN0608	1.00	-0.114	0.000	0.000	0.000
JN0609	1.00	-0.132	0.000	0.000	0.000
JN06010	2.00	0.785	0.000	0.000	0.000
JN06011	1.00	-0.080	0.000	0.000	0.000
JN06012	1.00	-0.202	0.000	0.000	0.000
JN06013	1.00	-0.277	0.000	0.000	0.000
JN06E2	1.00	-0.259	0.000	0.000	0.000
JN06E6	1.00	-0.219	0.000	0.000	0.000
JN06G2	1.00	0.039	0.000	0.000	0.000
JN06G3	1.00	-0.097	0.000	0.000	0.000
JN06G4	1.00	-0.259	0.000	0.000	0.000
JN06G6	1.00	-0.185	0.000	0.000	0.000
JN06G7	1.00	-0.248	0.000	0.000	0.000
DE0701	1.00	-0.038	0.000	0.000	0.000
DE0705	1.00	-0.015	0.000	0.000	0.000
DE0706	1.00	-0.020	0.000	0.000	0.000
DE0708	2.00	0.804	0.000	0.000	0.000
DE0728	1.00	0.006	0.000	0.000	0.000
DE07210	2.00	0.049	0.000	0.000	0.000
DE07212	2.00	0.021	0.000	0.000	0.000
AG0801	1.00	-0.037	0.000	0.000	0.000
AG0807	1.00	-0.201	0.000	0.000	0.000
AG0809	1.00	-0.255	0.000	0.000	0.000
AG08011	1.00	-0.107	0.000	0.000	0.000
AG08012	1.00	-0.215	0.000	0.000	0.000

AG0823	1.00	-0.201	0.000	0.000	0.000
AG0824	1.00	-0.264	0.000	0.000	0.000
AG0827	1.00	0.087	0.000	0.000	0.000
AG08210	1.00	0.016	0.000	0.000	0.000
DE0801	1.00	-0.132	0.000	0.000	0.000
DE0803	2.00	0.117	0.000	0.000	0.000
DE0805	1.00	0.222	0.000	0.000	0.000
DE0822	1.00	-0.188	0.000	0.000	0.000
DE0823	1.00	0.023	0.000	0.000	0.000
DE0824	2.00	0.132	0.000	0.000	0.000
MY1141	1.00	-0.019	0.000	0.000	0.000
MY1146	1.00	-0.220	0.000	0.000	0.000
MY1148	2.00	0.338	0.000	0.000	0.000
MY1161	1.00	-0.052	0.000	0.000	0.000
MY1163	2.00	-0.157	0.000	0.000	0.000
MY1165	1.00	0.114	0.000	0.000	0.000
MY1169	1.00	-0.196	0.000	0.000	0.000
MY11611	1.00	0.240	0.000	0.000	0.000
MY11612	1.00	-0.334	0.000	0.000	0.000
JN0801	1.00	0.316	0.000	0.000	0.000
JN0802	1.00	-0.189	0.000	0.000	0.000
JN0804	1.00	-0.308	0.000	0.000	0.000
JN0806	2.00	1.023	0.000	0.000	0.000
JN0821	1.00	-0.110	0.000	0.000	0.000
JN0827	1.00	-0.037	0.000	0.000	0.000
JN0841	1.00	-0.127	0.000	0.000	0.000
JN0846	1.00	-0.201	0.000	0.000	0.000
JN0848	2.00	0.948	0.000	0.000	0.000
JN08410	1.00	0.046	0.000	0.000	0.000
JN0861	1.00	-0.322	0.000	0.000	0.000
JN0862	1.00	-0.160	0.000	0.000	0.000
JN0867	1.00	-0.188	0.000	0.000	0.000
JN0869	1.00	-0.122	0.000	0.000	0.000
JN08611	1.00	-0.159	0.000	0.000	0.000
JN08614	1.00	0.069	0.000	0.000	0.000
JN08615	1.00	0.593	0.000	0.000	0.000
AG1001	2.00	0.243	0.000	0.000	0.000
AG1002	1.00	-0.166	0.000	0.000	0.000
MY1101	1.00	-0.145	0.000	0.000	0.000
MY1103	1.00	-0.081	0.000	0.000	0.000
MY1104	1.00	-0.087	0.000	0.000	0.000
MY1105	1.00	-0.085	0.000	0.000	0.000
MY1123	1.00	-0.046	0.000	0.000	0.000
MY1124	2.00	0.819	0.000	0.000	0.000
MY1125	1.00	-0.239	0.000	0.000	0.000
JN1249	1.00	-0.272	0.000	0.000	0.000
JN12411	1.00	0.051	0.000	0.000	0.000
MY1101	1.00	-0.274	0.000	0.000	0.000
MY1104	1.00	-0.242	0.000	0.000	0.000
MY1105	1.00	-0.165	0.000	0.000	0.000
MY1107	1.00	-0.300	0.000	0.000	0.000
MY11015	1.00	-0.058	0.000	0.000	0.000
MY11016	1.00	-0.248	0.000	0.000	0.000
MY1122	1.00	0.205	0.000	0.000	0.000

MY1123	1.00	-0.270	0.000	0.000	0.000
MY1125	1.00	-0.283	0.000	0.000	0.000
MY1128	1.00	0.740	0.000	0.000	0.000
MY1142	1.00	-0.294	0.000	0.000	0.000
MY1161	1.00	-0.300	0.000	0.000	0.000
MY1162	1.00	-0.078	0.000	0.000	0.000
MY1163	1.00	-0.202	0.000	0.000	0.000
MY1164	1.00	-0.247	0.000	0.000	0.000
MY1165	1.00	0.102	0.000	0.000	0.000
JN13C1	1.00	0.241	0.000	0.000	0.000
JN13C3	1.00	-0.305	0.000	0.000	0.000
JN13C4	1.00	0.378	0.000	0.000	0.000
JN13C6	1.00	0.257	0.000	0.000	0.000
JN13E2	1.00	-0.259	0.000	0.000	0.000
JN13E3	2.00	0.220	0.000	0.000	0.000
JN13E4	1.00	-0.303	0.000	0.000	0.000
JN13E6	1.00	-0.137	0.000	0.000	0.000
JN1302	1.00	-0.067	0.000	0.000	0.000
JN1325	1.00	-0.269	0.000	0.000	0.000
JN1327	1.00	0.051	0.000	0.000	0.000
JN1329	1.00	0.608	0.000	0.000	0.000
JN1341	1.00	-0.182	0.000	0.000	0.000
JN1342	1.00	-0.250	0.000	0.000	0.000
JN1346	1.00	-0.297	0.000	0.000	0.000
JN1348	1.00	-0.127	0.000	0.000	0.000
JN1349	1.00	-0.182	0.000	0.000	0.000
JN13410	1.00	-0.179	0.000	0.000	0.000
JN13411	1.00	-0.174	0.000	0.000	0.000
JN13414	1.00	-0.134	0.000	0.000	0.000
JN13415	1.00	-0.157	0.000	0.000	0.000
JN1383	1.00	0.429	0.000	0.000	0.000
JN1386	1.00	-0.187	0.000	0.000	0.000
JN13A2	1.00	-0.182	0.000	0.000	0.000
JN13A3	1.00	0.597	0.000	0.000	0.000
JN13A4	1.00	-0.305	0.000	0.000	0.000
JN13A5	1.00	-0.090	0.000	0.000	0.000
JN13A6	1.00	-0.110	0.000	0.000	0.000
JN13A7	1.00	-0.146	0.000	0.000	0.000
JN13A8	1.00	-0.297	0.000	0.000	0.000
JN13A9	1.00	-0.174	0.000	0.000	0.000
JN13A10	1.00	-0.179	0.000	0.000	0.000
JN13A11	1.00	-0.157	0.000	0.000	0.000
NO1541	1.00	-0.175	0.000	0.000	0.000
NO1543	1.00	-0.054	0.000	0.000	0.000
NO1545	1.00	0.037	0.000	0.000	0.000
NO1548	1.00	0.268	0.000	0.000	0.000
NO1561	1.00	-0.126	0.000	0.000	0.000
NO1566	1.00	-0.153	0.000	0.000	0.000
NO1569	2.00	0.626	0.000	0.000	0.000
OC1602	1.00	-0.071	0.000	0.000	0.000
OC1604	1.00	-0.129	0.000	0.000	0.000
OC1606	1.00	0.397	0.000	0.000	0.000
OC1608	1.00	0.580	0.000	0.000	0.000
OC1609	1.00	-0.036	0.000	0.000	0.000

OC16010	1.00	0.101	0.000	0.000	0.000
JN13I2	2.00	0.438	0.000	0.000	0.000
JN13I5	1.00	-0.152	0.000	0.000	0.000
JN13I6	1.00	-0.132	0.000	0.000	0.000
JN13I7	1.00	-0.229	0.000	0.000	0.000
JN13I8	1.00	0.089	0.000	0.000	0.000
NO1401	1.00	-0.067	0.000	0.000	0.000
NO1403	1.00	0.091	0.000	0.000	0.000
NO1405	1.00	-0.143	0.000	0.000	0.000
NO1406	1.00	-0.085	0.000	0.000	0.000
NO1407	1.00	0.160	0.000	0.000	0.000
NO1408	2.00	1.764	0.000	0.000	0.000
NO1422	1.00	0.090	0.000	0.000	0.000
NO1424	1.00	-0.063	0.000	0.000	0.000
NO1425	1.00	-0.110	0.000	0.000	0.000
NO1427	2.00	0.619	0.000	0.000	0.000
NO1501	1.00	-0.192	0.000	0.000	0.000
NO1502	1.00	0.041	0.000	0.000	0.000
NO1503	1.00	-0.162	0.000	0.000	0.000
NO1504	1.00	-0.117	0.000	0.000	0.000
NO1505	1.00	0.096	0.000	0.000	0.000
NO1506	2.00	1.738	0.000	0.000	0.000
NO1507	1.00	0.250	0.000	0.000	0.000
NO1523	1.00	-0.126	0.000	0.000	0.000
NO1524	1.00	-0.179	0.000	0.000	0.000
NO1525	2.00	0.626	0.000	0.000	0.000
NO1526	1.00	-0.117	0.000	0.000	0.000
JL2304	1.00	0.249	0.000	0.000	0.000
JL2306	1.00	-0.277	0.000	0.000	0.000
JL2322	1.00	-0.150	0.000	0.000	0.000
JL2323	1.00	-0.102	0.000	0.000	0.000
JL2326	1.00	-0.037	0.000	0.000	0.000
MY2401	1.00	-0.183	0.000	0.000	0.000
MY2403	1.00	-0.220	0.000	0.000	0.000
MY2404	1.00	-0.120	0.000	0.000	0.000
MY2405	1.00	-0.291	0.000	0.000	0.000
MY2406	1.00	-0.110	0.000	0.000	0.000
MY2408	1.00	0.006	0.000	0.000	0.000
MY24011	1.00	-0.195	0.000	0.000	0.000
MY24012	1.00	-0.130	0.000	0.000	0.000
MY2424	1.00	-0.220	0.000	0.000	0.000
MY2425	1.00	-0.044	0.000	0.000	0.000
MY2426	1.00	-0.369	0.000	0.000	0.000
MY2429	1.00	-0.255	0.000	0.000	0.000
MY24213	1.00	-0.189	0.000	0.000	0.000
MY24215	1.00	-0.314	0.000	0.000	0.000
MY24216	1.00	-0.221	0.000	0.000	0.000
MY24217	1.00	-0.114	0.000	0.000	0.000
MY24219	1.00	-0.229	0.000	0.000	0.000
JL2102	1.00	-0.232	0.000	0.000	0.000
JL2123	1.00	-0.163	0.000	0.000	0.000
JL2124	1.00	-0.021	0.000	0.000	0.000
JL2125	1.00	-0.187	0.000	0.000	0.000
JL2127	1.00	-0.125	0.000	0.000	0.000

JL2128	1.00	-0.187	0.000	0.000	0.000
JL2129	1.00	-0.285	0.000	0.000	0.000
JL21211	1.00	-0.271	0.000	0.000	0.000
JL2142	1.00	-0.224	0.000	0.000	0.000
JL2143	1.00	-0.119	0.000	0.000	0.000
JL2145	1.00	-0.090	0.000	0.000	0.000
NO2623	1.00	0.015	0.000	0.000	0.000
NO2626	2.00	1.905	0.000	0.000	0.000
NO2643	2.00	1.688	0.000	0.000	0.000
SE2605	2.00	0.061	0.000	0.000	0.000
SE2606	1.00	-0.075	0.000	0.000	0.000
SE26010	1.00	-0.078	0.000	0.000	0.000
SE2624	1.00	-0.058	0.000	0.000	0.000
SE2627	1.00	-0.020	0.000	0.000	0.000
SE2629	1.00	-0.176	0.000	0.000	0.000
SE26211	1.00	0.176	0.000	0.000	0.000
MY2441	1.00	-0.155	0.000	0.000	0.000
MY2443	1.00	-0.076	0.000	0.000	0.000
MY2444	1.00	-0.079	0.000	0.000	0.000
MY2448	1.00	-0.009	0.000	0.000	0.000
MY2449	1.00	-0.219	0.000	0.000	0.000
MY24410	1.00	-0.247	0.000	0.000	0.000
MY24412	1.00	-0.040	0.000	0.000	0.000
MY24414	1.00	-0.293	0.000	0.000	0.000
MY24415	1.00	0.043	0.000	0.000	0.000
AP2607	1.00	-0.195	0.000	0.000	0.000
AP2608	1.00	-0.313	0.000	0.000	0.000
AP2628	1.00	-0.233	0.000	0.000	0.000
AP26210	1.00	-0.117	0.000	0.000	0.000
AP26211	1.00	-0.348	0.000	0.000	0.000
NO2601	1.00	0.045	0.000	0.000	0.000
NO2603	1.00	0.032	0.000	0.000	0.000
NO2604	1.00	0.161	0.000	0.000	0.000
NO2606	1.00	-0.054	0.000	0.000	0.000
NO2607	2.00	1.884	0.000	0.000	0.000
NO2608	2.00	1.854	0.000	0.000	0.000
JL3002	1.00	-0.056	0.000	0.000	0.000
JL3006	1.00	0.017	0.000	0.000	0.000
JL3024	1.00	-0.157	0.000	0.000	0.000
JL3025	1.00	-0.276	0.000	0.000	0.000
JL3027	1.00	-0.220	0.000	0.000	0.000
MY3003	1.00	0.097	0.000	0.000	0.000
MY3004	1.00	-0.082	0.000	0.000	0.000
MY3026	1.00	0.511	0.000	0.000	0.000
MY3027	1.00	-0.192	0.000	0.000	0.000
MY3028	1.00	-0.028	0.000	0.000	0.000
MY3029	1.00	-0.285	0.000	0.000	0.000
MY30210	2.00	0.022	0.000	0.000	0.000
SE2802	1.00	-0.063	0.000	0.000	0.000
SE2806	1.00	-0.069	0.000	0.000	0.000
SE2807	1.00	-0.082	0.000	0.000	0.000
SE2808	1.00	-0.056	0.000	0.000	0.000
SE2821	1.00	0.011	0.000	0.000	0.000
SE2822	1.00	-0.184	0.000	0.000	0.000

SE2841	1.00	0.090	0.000	0.000	0.000
SE2846	1.00	-0.133	0.000	0.000	0.000
JL3121	1.00	0.160	0.000	0.000	0.000
JL3123	1.00	0.550	0.000	0.000	0.000
JL3124	1.00	0.188	0.000	0.000	0.000
JN0114	1.00	-0.172	0.000	0.000	0.000
JN0115	1.00	-0.068	0.000	0.000	0.000
JN0116	1.00	-0.040	0.000	0.000	0.000
JN0117	1.00	-0.184	0.000	0.000	0.000
JN0131	1.00	-0.193	0.000	0.000	0.000
JN0134	1.00	-0.149	0.000	0.000	0.000
JN0135	1.00	0.045	0.000	0.000	0.000
JN0136	1.00	-0.106	0.000	0.000	0.000
JN0139	1.00	0.331	0.000	0.000	0.000
JN01310	1.00	-0.029	0.000	0.000	0.000
JN01311	1.00	-0.144	0.000	0.000	0.000
JN01313	1.00	0.022	0.000	0.000	0.000
JN01314	1.00	0.071	0.000	0.000	0.000
JN01H3	1.00	0.374	0.000	0.000	0.000
JN01H5	1.00	-0.310	0.000	0.000	0.000
JN01H6	1.00	-0.289	0.000	0.000	0.000
JN01H13	1.00	-0.263	0.000	0.000	0.000
MY3041	1.00	-0.099	0.000	0.000	0.000
MY3044	1.00	-0.111	0.000	0.000	0.000
MY3045	1.00	0.168	0.000	0.000	0.000
MY3046	2.00	1.229	0.000	0.000	0.000
MY3048	1.00	-0.274	0.000	0.000	0.000
MY3061	1.00	0.081	0.000	0.000	0.000
MY3062	1.00	0.151	0.000	0.000	0.000
MY3065	1.00	-0.099	0.000	0.000	0.000
MY3067	1.00	-0.225	0.000	0.000	0.000
MY3068	2.00	1.179	0.000	0.000	0.000
MY3069	2.00	1.155	0.000	0.000	0.000
MY30610	1.00	-0.270	0.000	0.000	0.000
JL31015	1.00	0.839	0.000	0.000	0.000
MY1011	1.00	-0.179	0.000	0.000	0.000
MY1012	1.00	0.004	0.000	0.000	0.000
MY1013	1.00	-0.041	0.000	0.000	0.000
MY1014	2.00	0.999	0.000	0.000	0.000
MY1031	1.00	-0.109	0.000	0.000	0.000
MY1034	1.00	-0.172	0.000	0.000	0.000
MY1036	1.00	-0.179	0.000	0.000	0.000
MY1038	1.00	0.085	0.000	0.000	0.000
MY10310	1.00	-0.192	0.000	0.000	0.000
MY10312	1.00	0.138	0.000	0.000	0.000
MY1056	2.00	0.452	0.000	0.000	0.000
MY1057	1.00	-0.179	0.000	0.000	0.000
MY1059	1.00	0.088	0.000	0.000	0.000
MY10510	1.00	-0.212	0.000	0.000	0.000
MY1071	1.00	0.087	0.000	0.000	0.000
MY1072	1.00	-0.244	0.000	0.000	0.000
MY1075	2.00	0.437	0.000	0.000	0.000
MY1077	2.00	-0.061	0.000	0.000	0.000
MY1078	1.00	0.086	0.000	0.000	0.000

MY1079	1.00	-0.212	0.000	0.000	0.000
JN1112	1.00	-0.093	0.000	0.000	0.000
JN1114	1.00	-0.238	0.000	0.000	0.000
JN1116	1.00	-0.043	0.000	0.000	0.000
JN1118	1.00	-0.265	0.000	0.000	0.000
JN1119	1.00	0.032	0.000	0.000	0.000
JN11114	1.00	-0.061	0.000	0.000	0.000
JN1131	1.00	0.136	0.000	0.000	0.000
JN1133	1.00	-0.118	0.000	0.000	0.000
JN1134	1.00	0.497	0.000	0.000	0.000
JN1135	1.00	-0.222	0.000	0.000	0.000
JN1136	1.00	-0.300	0.000	0.000	0.000
JN1138	1.00	-0.007	0.000	0.000	0.000
JN1139	1.00	-0.288	0.000	0.000	0.000
JN01J2	1.00	-0.045	0.000	0.000	0.000
JN01J3	1.00	-0.167	0.000	0.000	0.000
JN01J4	1.00	0.120	0.000	0.000	0.000
JN0911	2.00	0.373	0.000	0.000	0.000
JN0912	1.00	-0.048	0.000	0.000	0.000
JN0913	1.00	-0.325	0.000	0.000	0.000
JN0914	1.00	-0.231	0.000	0.000	0.000
JN0916	1.00	0.081	0.000	0.000	0.000
JN0917	1.00	-0.192	0.000	0.000	0.000
JN0918	1.00	0.017	0.000	0.000	0.000
JN09112	1.00	-0.137	0.000	0.000	0.000
JN09113	1.00	-0.199	0.000	0.000	0.000
JN0937	1.00	-0.242	0.000	0.000	0.000
JN0938	1.00	-0.316	0.000	0.000	0.000
JN09310	1.00	-0.096	0.000	0.000	0.000
MY1116	1.00	0.056	0.000	0.000	0.000
MY1118	1.00	-0.291	0.000	0.000	0.000
MY11110	2.00	1.262	0.000	0.000	0.000
MY1131	1.00	-0.020	0.000	0.000	0.000
MY1132	1.00	-0.102	0.000	0.000	0.000
MY1133	1.00	0.051	0.000	0.000	0.000
MY1151	2.00	0.166	0.000	0.000	0.000
MY1152	1.00	0.051	0.000	0.000	0.000
MY1154	2.00	0.228	0.000	0.000	0.000
MY1156	2.00	0.550	0.000	0.000	0.000
MY1172	1.00	-0.261	0.000	0.000	0.000
MY1173	1.00	-0.159	0.000	0.000	0.000
MY1174	2.00	-0.204	0.000	0.000	0.000
MY1175	1.00	-0.145	0.000	0.000	0.000
MY1176	1.00	-0.078	0.000	0.000	0.000
MY1177	2.00	1.248	0.000	0.000	0.000
MY1179	1.00	-0.140	0.000	0.000	0.000
MY11710	1.00	-0.202	0.000	0.000	0.000
MY11713	1.00	-0.205	0.000	0.000	0.000
MY11714	1.00	0.041	0.000	0.000	0.000
MY11F1	1.00	0.010	0.000	0.000	0.000
MY11F2	2.00	0.844	0.000	0.000	0.000
MY11H1	1.00	0.237	0.000	0.000	0.000
MY11H3	1.00	0.179	0.000	0.000	0.000
MY11H4	1.00	-0.127	0.000	0.000	0.000

MY11H6	2.00	-0.036	0.000	0.000	0.000
MY11H8	2.00	0.067	0.000	0.000	0.000
MY11H10	1.00	0.172	0.000	0.000	0.000
MY11H14	2.00	0.037	0.000	0.000	0.000
MY11H15	2.00	0.847	0.000	0.000	0.000
JN1174	1.00	-0.157	0.000	0.000	0.000
SE1612	1.00	-0.255	0.000	0.000	0.000
SE1613	2.00	0.870	0.000	0.000	0.000
SE1614	1.00	-0.268	0.000	0.000	0.000
SE1616	1.00	-0.174	0.000	0.000	0.000
SE1617	1.00	-0.080	0.000	0.000	0.00S
SE1631	1.00	-0.143	0.000	0.000	0.000
SE1632	1.00	0.242	0.000	0.000	0.000
SE1633	1.00	0.906	0.000	0.000	0.000
SE1634	1.00	0.200	0.000	0.000	0.000
SE1638	1.00	-0.085	0.000	0.000	0.000
SE16310	1.00	0.031	0.000	0.000	0.000
SE16311	1.00	0.239	0.000	0.000	0.000
SE16313	1.00	-0.194	0.000	0.000	0.000
SE16314	1.00	-0.151	0.000	0.000	0.000
JN3011	1.00	-0.182	0.000	0.000	0.000
JN3012	1.00	-0.211	0.000	0.000	0.000
JN3013	1.00	-0.038	0.000	0.000	0.000
JN3015	1.00	-0.040	0.000	0.000	0.000
JN3016	1.00	-0.280	0.000	0.000	0.000
JN30112	1.00	-0.220	0.000	0.000	0.000
JN30113	1.00	-0.190	0.000	0.000	0.000
JN3031	1.00	-0.208	0.000	0.000	0.000
JN3035	1.00	-0.217	0.000	0.000	0.000
JN3036	1.00	0.399	0.000	0.000	0.000
JN3051	1.00	-0.099	0.000	0.000	0.000
JN3055	1.00	-0.241	0.000	0.000	0.000
JN3056	2.00	-0.164	0.000	0.000	0.000
JN3076	1.00	-0.241	0.000	0.000	0.000
JN3077	2.00	-0.164	0.000	0.000	0.000
JN3091	1.00	-0.231	0.000	0.000	0.000
JN3092	1.00	-0.176	0.000	0.000	0.000
JN3094	1.00	-0.172	0.000	0.000	0.000
JN3096	1.00	-0.098	0.000	0.000	0.000
JN30912	1.00	0.271	0.000	0.000	0.000
JN30915	1.00	-0.085	0.000	0.000	0.000
JN30916	1.00	-0.175	0.000	0.000	0.000
JN30917	1.00	-0.092	0.000	0.000	0.000
MY11J2	1.00	-0.212	0.000	0.000	0.000
MY11J4	1.00	0.210	0.000	0.000	0.000
MY11J6	1.00	-0.107	0.000	0.000	0.000
MY11J7	1.00	-0.078	0.000	0.000	0.000
MY11J9	1.00	-0.239	0.000	0.000	0.000
MY11L1	1.00	-0.258	0.000	0.000	0.000
MY11L3	2.00	-0.099	0.000	0.000	0.000
MY11L8	1.00	-0.212	0.000	0.000	0.000
MY11L10	1.00	-0.138	0.000	0.000	0.000
MY11L13	1.00	-0.383	0.000	0.000	0.000
JL0421	1.00	-0.190	0.000	0.000	0.000

JL0423	1.00	-0.224	0.000	0.000	0.000
JL0428	2.00	1.516	0.000	0.000	0.000
JL04211	1.00	-0.220	0.000	0.000	0.000
AP29E1	1.00	-0.195	0.000	0.000	0.000
AP29E4	1.00	-0.192	0.000	0.000	0.000
AP29E6	1.00	0.043	0.000	0.000	0.000
AP29E9	1.00	-0.277	0.000	0.000	0.000
AP29E11	1.00	-0.303	0.000	0.000	0.000
AP29E12	1.00	-0.351	0.000	0.000	0.000
AP29E14	1.00	0.174	0.000	0.000	0.000
AP29E16	1.00	-0.169	0.000	0.000	0.000
JN1151	1.00	-0.072	0.000	0.000	0.000
JN1153	1.00	-0.225	0.000	0.000	0.000
JN1155	1.00	0.003	0.000	0.000	0.000
JN1156	1.00	-0.088	0.000	0.000	0.000
JN01F2	1.00	-0.290	0.000	0.000	0.000
JN01F3	1.00	-0.215	0.000	0.000	0.000
JN01F7	2.00	0.791	0.000	0.000	0.000
JN01F8	1.00	-0.176	0.000	0.000	0.000
JN01F11	1.00	-0.345	0.000	0.000	0.000
JN01F12	1.00	-0.365	0.000	0.000	0.000
AP2802	1.00	-0.251	0.000	0.000	0.000
AP2803	1.00	-0.191	0.000	0.000	0.000
AP2804	1.00	-0.190	0.000	0.000	0.000
AP2806	1.00	-0.001	0.000	0.000	0.000
AP28012	1.00	0.021	0.000	0.000	0.000
AP28013	1.00	-0.023	0.000	0.000	0.000
AP28016	1.00	-0.253	0.000	0.000	0.000
AP28020	1.00	-0.145	0.000	0.000	0.000
AP28023	1.00	0.036	0.000	0.000	0.000
AP28025	1.00	-0.229	0.000	0.000	0.000
AP28026	1.00	-0.165	0.000	0.000	0.000
AP2307	1.00	-0.204	0.000	0.000	0.000
AP23011	1.00	-0.094	0.000	0.000	0.000
AP23013	1.00	-0.198	0.000	0.000	0.000
AP23015	2.00	-0.138	0.000	0.000	0.000
AP2201	1.00	-0.214	0.000	0.000	0.000
AP2202	1.00	-0.003	0.000	0.000	0.000
AP2205	1.00	0.372	0.000	0.000	0.000
AP2207	1.00	0.009	0.000	0.000	0.000
JN1226	1.00	0.025	0.000	0.000	0.000
N06I3	1.00	0.033	0.000	0.000	0.000
JN06I5	1.00	0.657	0.000	0.000	0.000
JN06I6	1.00	0.063	0.000	0.000	0.000
JN06I7	1.00	-0.080	0.000	0.000	0.000
JN06I10	1.00	-0.214	0.000	0.000	0.000
MY0521	1.00	-0.149	0.000	0.000	0.000
MY0522	1.00	-0.280	0.000	0.000	0.000
MY0525	1.00	-0.290	0.000	0.000	0.000
MY0527	1.00	-0.144	0.000	0.000	0.000
MY0501	2.00	0.400	0.000	0.000	0.000
MY0504	1.00	-0.087	0.000	0.000	0.000
MY0506	1.00	0.604	0.000	0.000	0.000